Maneuvering Formations of Mobile Agents Using Designed Mismatched Angles

Liangming Chen, *Graduate Student Member, IEEE*, Hector Garcia de Marina, *Member, IEEE*, and Ming Cao, *Senior Member, IEEE*

***Abstract*—This article investigates how to maneuver a planar formation of mobile agents using designed mismatched angles. The desired formation shape is specified by a set of interior angle constraints. To realize the maneuver of translation, rotation, and scaling of the formation as a whole, we intentionally force the agents to maintain mismatched desired angles by introducing a pair of mismatch parameters for each angle constraint. To allow different information requirements in the design and implementation stages, we consider both measurement-dependent and measurement-independent mismatches. Starting from a triangular formation, we consider generically angle rigid formations that can be constructed from the triangular formation by adding new agents in sequence, each having two angle constraints associated with some existing three agents. The control law for each newly added agent arises naturally from the angle constraints and makes full use of the angle mismatch parameters. We show that the control can effectively stabilize the formations while simultaneously realizing maneuvering. Simulations are conducted to validate the theoretical results.**

***Index Terms*—Angle rigid formation, designed mismatched angles, formation maneuvering, multiagent systems.**

I. Introduction

MULTIAGENT formations have recently attracted attention because of the broad applications in, e.g., search and rescue of unmanned aerial vehicles [1], coordination of multiple mobile manipulators [2], and satellite formation flying [3]. Both formation shape control and formation maneuvering have been studied [4], [5]. The works in [5]–[7] realized the control of desired formation shapes by using the measurements of relative positions, distances, and bearings, respectively. At the same time, in many practical applications, formations are expected to be "maneuverable," e.g., capable of translating, scaling, and rotating to adapt to complex environments. For instance, when a team of flying unmanned aerial vehicles aims at going through some areas containing obstacles, they need to change the velocity, orientation, and even the scale of the whole formation. Therefore, researchers have studied the formation maneuvering problem that requires the achievement of not only the desired formation shape but also simultaneously the translation, rotation, or scaling of the formation [8].

To achieve formation maneuvering, some researchers have proposed several approaches given different types of formation shape descriptions and available sensing information. When a desired formation shape is described by relative positions, formation translation was achieved in [9]. For rigid formations with distance constraints, the rotational and translational formation maneuvering algorithms were designed in [10] and [11] by introducing a pair of mismatches per distance constraint. For a desired formation shape described by interagent bearings, based on the bearing rigidity developed in [7], the work in [8] achieved the scaling and translational formation maneuvering using relative position measurements. Note that these works [8]–[11] cannot fully achieve the formation maneuvering of scaling, rotation, and translation easily at the same time. The reason is that, because of the dependence of coordinate frames, displacement constraints vary during rotation and scaling, distance constraints vary during scaling, and bearing constraints vary during rotation. To maneuver the formation with the capacity of translation, rotation, and scaling, some other approaches were proposed [12]–[16]. Note that for most of the proposed formation maneuvering algorithms [8]–[17], the measurements of relative positions are required. Compared with relative position measurements, bearing measurements are cheaper, more reliable, and accessible that can be obtained from the passive radars, sonar systems, or cameras [18], [19].

Motivated by the facts that interior angle constraints are invariant during translation, rotation, and scaling, this article aims at realizing the formation maneuvering enabling translation, rotation, and scaling, under the conditions that the formation shape is described by interior angle constraints and the measurements are chosen bearings. To be more specific, based on the angle-based formation stabilization law [20], [21], we employ mismatches in prescribed angles, and propose to use "designed mismatched

Manuscript received June 17, 2020; revised January 11, 2021; accepted February 27, 2021. Date of publication March 17, 2021; date of current version March 29, 2022. The work of Hector Garcia de Marina was supported by the *Atraccion de Talento* Grant 2019-T2/TIC-13503 from the Government of the Autonomous Community of Madrid. The work of Ming Cao was supported in part by the European Research Council under Grant ERC-CoG-771687 and in part by the Netherlands Organization for Scientific Research under Grant NWO-vidi-14134. Recommended by Associate Editor G. Notarstefano. *(Corresponding author: Liangming Chen.)*

Liangming Chen and Ming Cao are with the Faculty of Science and Engineering, University of Groningen, Groningen 9747 AG, The Netherlands (e-mail: liangmingchen2018@gmail.com; ming.cao@ieee.org).

Hector Garcia de Marina is with the Department of Computer Architecture and Automatic Control, Faculty of Physics Universidad Complutense de Madrid, Madrid 28040, Spain (e-mail: hgarciad@ucm.es).

Color versions of one or more figures in this article are available at https://doi.org/10.1109/TAC.2021.3066388.

Digital Object Identifier 10.1109/TAC.2021.3066388

angles" after the angle mismatches are added to each agent's desired interior angles. We first consider the maneuvering of three-agent formation. The mismatches that we consider can be either measurement dependent or measurement independent in the sense that the former depends on the current measurements between neighboring agents, and the latter does not. To grow a triangular formation into a large angle rigid formation, two angle constraints associated with three existing agents are required for each sequentially added agent, which naturally gives rise to the formation maneuver control algorithm for the newly added agents.

The contributions of this article can be summarized as follows. The formation maneuver control is realized enabling translation, rotation, and scaling using the bearing measurements. Both the measurement-dependent and measurement-independent mismatch cases are studied. When the mismatches are measurement-independent, the formation maneuvering algorithm only needs the information of the desired formation shape in the design stage and only local bearing measurements in the implementation stage.

The rest of this article is organized as follows. Section II gives the problem formulation. Section III gives the results for triangular formation maneuver. In Section IV, we present the extension from triangular formation to generically angle rigid formation. Simulation results are shown in Section V, and finally, Section VI concludes this article.

II. Problem Formulation

A. Agents' Dynamics

For an N-agent system moving in the plane, the motion dynamics of its agent i are governed by

$$\dot{p}_i = u_i, i = 1, \ldots, N \tag{1}$$

where $p_i \in \mathbb{R}^2$ denotes the position of the agent i described in a fixed global coordinate frame $\sum_g$, and $u_i \in \mathbb{R}^2$ is the control input to be designed.

B. Bearing Measurements

Each agent i has its own fixed coordinate frame $\sum_i$, which may differ from $\sum_g$. Let p_j^i denote agent j's position in $\sum_i$. To simplify notation, whenever causing no confusion, we drop the superscript reference to $\sum_g$, e.g., $p_i = p_i^g$. The agent i measures the bearing $\phi_{ij} \in [0, 2\pi)\, \forall j \in \mathcal{N}_i$ toward the agent j evaluated counter-clockwise from the X-axis of $\sum_i$, and here, $\mathcal{N}_i$ denotes the set of the neighbors of the agent i that do not coincide with i. We also call the unit vector $z_{ij}^i := \frac{p_j^i - p_i^i}{\|p_j^i - p_i^i\|} = \begin{bmatrix} \cos\phi_{ij} \\ \sin\phi_{ij} \end{bmatrix}$ the bearing from i to j, which starts from p_i^i, points toward p_j^i, and can be uniquely determined by ϕ_{ij}. For the agents $i, i+1$, and $i-1$ shown in Fig. 1, the interior angle α_i can be calculated by

$$\alpha_i := \measuredangle(i-1)i(i+1) = \arccos(z_{i(i+1)}^\top z_{i(i-1)}). \tag{2}$$

Note that even when $\sum_i$ are chosen differently, α_i remains the same but $z_{ij}^g = R_i^g z_{ij}^i$, where z_{ij}^g is the bearing from p_i to p_j described in $\sum_g$, and $R_i^g \in SO(2)$ denotes the rotation matrix from $\sum_i$ to $\sum_g$.

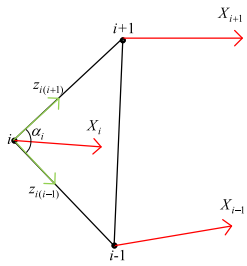

Fig. 1. Bearing measurements.

C. Problem Formulation

The goal of this article is to design the control input u_i in (1) for each agent i such that the N-agent system achieves a desired formation described by interior angles, and at the same time, realizes desired maneuvering. First, we study the triangular case when $N = 3$, and then, extend the obtained results to generically angle rigid formations when $N > 3$. For the triangular case $N = 3$, the objectives are as follows:

1) to achieve the desired triangular formation shape, i.e.,

$$\lim_{t\to\infty} e_i(t) = 0, \forall i = 1, 2, 3 \tag{3}$$

where the formation-shape error signal e_i are defined to be $e_i(t) = \alpha_i(t) - \alpha_i^*$, $\alpha_i^* \in (0, \pi)$ denotes agent i's desired interior angle, and naturally $\alpha_1^* + \alpha_2^* + \alpha_3^* = \pi$;

2) to achieve one of the following separately defined maneuvering:

a) translational formation maneuver

$$\lim_{t\to\infty}(\dot{p}_i(t) - v_c^*) = 0 \quad \forall i = 1, 2, 3 \tag{4}$$

where $v_c^* \in \mathbb{R}^2$ is the desired translational velocity described in $\sum_g$;

b) rotational formation maneuver

$$\lim_{t\to\infty}(\dot{p}_i(t) - \omega^* E p_{ci}(t)) = 0 \tag{5}$$

where $E = \begin{bmatrix} 0 & -1 \\ 1 & 0 \end{bmatrix}$ is a skew-symmetric matrix, $p_{ci} = p_i - p_c$ denotes the vector from the maneuvering reference point p_c to agent i's position p_i (thus, Ep_{ci} corresponding to rotating p_{ci} by $\pi/2$ counter clockwise), and $\omega^* \in \mathbb{R}$ is the desired rotational angular speed, with $\omega^* > 0$ corresponding to rotating counter-clockwise. The formation reference point p_c can have different choices, e.g., the centroid $p_c = \frac{1}{N}\sum_{i=1}^N p_i$; in applications, it can be chosen to be the position of a well-recognized landmark in the environment.

c) scaling formation maneuver

$$\lim_{t\to\infty}(\dot{p}_i(t) - s(t)p_{ci}(t)) = 0 \tag{6}$$

where $s(t) \in \mathbb{R}$ is the modulation factor for the scaling speed, which can be typically chosen as $s(t) = k_s e^{-\gamma t}, \gamma > 0, k_s \in \mathbb{R}$. Note that $s(t) > 0$ or $k_s > 0$ corresponds to enlarging the formation, while $s(t) < 0$ or $k_s < 0$ shrinking the formation.

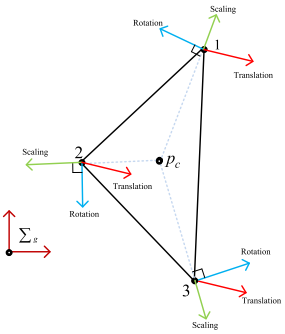

Fig. 2. Formation maneuver velocity vectors: translation, rotation, and scaling.

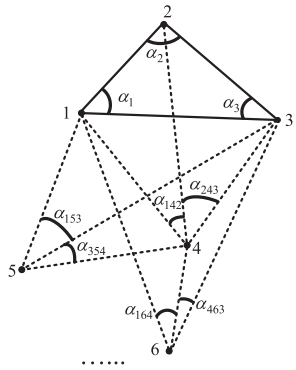

Fig. 3. Formation growing method from a triangular shape.

If the translation, rotation, and scaling maneuverings are required to be achieved simultaneously, then by combining (4)–(6) together, the maneuvering control objective becomes

$$\lim_{t\to\infty}\left[\dot{p}_i(t)-(v_c^*+\omega^* E p_{ci}(t)+s(t)p_{ci}(t))\right]=0. \quad (7)$$

Note that when the formation reaches its desired shape, the motion of the formation as a whole can be decomposed into independent translation, rotation, and scaling [22, Sec. 4.6]. Therefore, the desired translation, rotation, and scaling motions can be achieved when (7) holds.

When $N>3$, we aim to control those multiagent formations that are angle rigid. Here, we briefly mention a few concepts from the angle rigidity theory. The multipoint framework that we consider consists of a set of points and angle constraints, and it is said to be *angle rigid* if under appropriately chosen angle constraints, the framework can only translate, rotate, or scale as a whole when one or more of its points are perturbed locally. An angle rigid multipoint framework with generic configuration $p=[p_1^{\mathrm{T}},\ldots,p_N^{\mathrm{T}}]^{\mathrm{T}}\in\mathbb{R}^{2N}$, e.g., no three points are collinear and no four points are on a circle, is said to be *generically angle rigid*. For more details about angle rigidity, readers can refer to [20].

To construct a generically angle rigid N-agent formation, according to [20], one can grow the formation by $N-2$ steps.

Step 1: One constructs the first triangular formation $\triangle 123$ using three angle constraints: $\measuredangle 123, \measuredangle 231, \measuredangle 312$.

Step 2: One adds agent 4 under the two angle constraints: $\measuredangle 142$ and $\measuredangle 243$.

...

Step $k-2$: One adds agent k under the two angle constraints: $\measuredangle j_1 k j_2$ and $\measuredangle j_2 k j_3$, $j_1,j_2,j_3\in\{1,\ldots,k-1\}$.

...

Step $N-2$: One adds agent N under the two angle constraints: $\measuredangle i_1 N i_2$ and $\measuredangle i_2 N i_3$, for some distinct $i_1,i_2,i_3\in\{1,\ldots,N-1\}$.

To guarantee the uniqueness of each agent's position in Steps 2 to $N-2$ under the given two angle constraints, the following assumption is needed.

Assumption 1: In the aforementioned Step $k, k=2,\ldots,N-2$ with the corresponding newly added agent i and its angle constraints $\measuredangle j_1 i j_2$ and $\measuredangle j_2 i j_3$, we assume that the positions of i, j_1, j_2, and j_3 are generic and no collinearity occurs, namely $\measuredangle j_1 i j_2\neq 0, \measuredangle j_1 i j_2\neq\pi$, and $\measuredangle j_2 i j_3\neq 0, \measuredangle j_2 i j_3\neq\pi$.

Remark 1: According to [20, Proposition 2], when i, j_1, j_2, and j_3 are generic as stipulated in Assumption 1, the position of each newly added agent $i, i=2,\ldots,N$ is locally uniquely determined by $\measuredangle j_1 i j_2$ and $\measuredangle j_2 i j_3$, which implies the angle rigidity of the constructed formation.

Then, for agents $i, i=4,\ldots,N$, the formation control objective is to achieve

$$\lim_{t\to\infty} e_{i1}(t)=\lim_{t\to\infty}(\alpha_{j_1 i j_2}(t)-\alpha^*_{j_1 i j_2})=0 \quad (8)$$

$$\lim_{t\to\infty} e_{i2}(t)=\lim_{t\to\infty}(\alpha_{j_2 i j_3}(t)-\alpha^*_{j_2 i j_3})=0 \quad (9)$$

where $j_1<i, j_2<i, j_3<i$, and $\alpha^*_{j_1 i j_2}\in(0,\pi), \alpha^*_{j_2 i j_3}\in(0,\pi)$ denote agent i's two desired angles formed with agents $j_1,j_2,j_3\in\{1,2,\ldots,i-1\}$, and to achieve the maneuvering of translation, rotation, and scaling as described in (4)–(6).

Therefore, the desired formation shape is described by a set of angle constraints $\alpha^*=\{\alpha_1^*,\alpha_2^*,\alpha_3^*,\alpha_{142}^*,\alpha_{243}^*,\ldots,\alpha^*_{j_1 k j_2},\alpha^*_{j_2 k j_3},\ldots,\alpha^*_{i_1 N i_2},\alpha^*_{i_2 N i_3}\}$. The goal is to achieve these angles and the maneuvering objective (7) simultaneously.

III. Triangular Formation Maneuver

In this section, we aim at achieving the triangular formation maneuvering for the first three agents. First, we will present a formation maneuver algorithm by introducing a pair of mismatches per angle constraint. Then, for the cases of measurement-dependent and measurement-independent mismatches, the formation maneuver control algorithms and the corresponding stability analysis will be given, respectively.

A. Formation Maneuver Algorithm Design

In [21], using bearing measurements, three agents achieved a triangular formation shape described by three interior angles $\alpha_i^*, i=1,2,3$. The control algorithms designed in [21] can be equivalently written as

$$u_i=-k_i(\alpha_i-\alpha_i^*)\frac{z_{i(i+1)}+z_{i(i-1)}}{\|z_{i(i+1)}+z_{i(i-1)}\|} \quad (10)$$

where $k_i>0$, $z_{i(i+1)}$ is the unit vector starting from p_i and pointing toward p_{i+1}, and this section considers that $(i+1)=$

1 when $i = 3$, and $(i-1) = 3$ when $i = 1$. In this article, we modify the control algorithm (10) into

$$u_i = -k_i(\alpha_i - \alpha_i^*)(z_{i(i+1)} + z_{i(i-1)}). \tag{11}$$

Now, we introduce a pair of designed-mismatches per angle constraint α_i^* in (11) such that the formation maneuvering with translation, rotation, and scaling can be realized. By following [23], we design the formation maneuvering law as

$$\begin{aligned} u_i &= -k_i\left(\alpha_i - \alpha_i^* - \frac{\mu_i}{k_i}\right) z_{i(i+1)} - k_i\left(\alpha_i - \alpha_i^* - \frac{\tilde{\mu}_i}{k_i}\right) z_{i(i-1)} \\ &= -k_i(\alpha_i - \alpha_i^*)[z_{i(i+1)} + z_{i(i-1)}] + [\mu_i z_{i(i+1)} + \tilde{\mu}_i z_{i(i-1)}] \\ &= u_{fi} + u_{mi} \end{aligned} \tag{12}$$

where $\mu_i \in \mathbb{R}$ and $\tilde{\mu}_i \in \mathbb{R}$ are the designed-mismatches associated with agent i's desired angle α_i^*, u_{fi} is the formation shape control part, and u_{mi} is the maneuver control part. From (7) and (12), the steady-state maneuver velocity $\dot{p}_i^*$ of the agent i at the desired triangular formation shape ($\alpha_i = \alpha_i^*$) should be decomposed into three parts as follows:

$$\begin{aligned} \dot{p}_i^* &= \dot{p}_{i(\text{translation})}^* + \dot{p}_{i(\text{rotation})}^* + \dot{p}_{i(\text{scaling})}^* \\ &= v_c^* + \omega^* E p_{ci} + s(t) p_{ci} = \mu_i z_{i(i+1)} + \tilde{\mu}_i z_{i(i-1)}. \end{aligned} \tag{13}$$

Note that in the aforementioned equation, $z_{i(i+1)}$ is determined by the bearing measurement $\phi_{i(i+1)}$, but p_{ci} is the vector from the reference point p_c to agent i's position p_i which needs to be additionally measured. In the following two subsections, we introduce two techniques to design the mismatches to realize the desired maneuvering, which are the measurement-dependent mismatches $\mu_i(z_{ij}, p_{ci})$, $\tilde{\mu}_i(z_{ij}, p_{ci})$ or $\mu_i(t)$, $\tilde{\mu}_i(t)$ for short that require the real-time measurements of $z_{ij}(t)$ and $p_{ci}(t)$, and the measurement-independent mismatches $\mu_i(\alpha^*)$, $\tilde{\mu}_i(\alpha^*)$ or μ_i, $\tilde{\mu}_i$ for short that are not related to the real-time measurements but calculated in the design stage based on the desired formation shape α^*.

B. Measurement-Dependent Mismatches

Now, we use the measurement-dependent mismatches to realize the desired maneuvering under the measurements of z_{ij} and p_{ci}, in which we assume that all the agents' coordinate frames $\sum_i$ have the same orientation as $\sum_g$. In the following, we first illustrate how to design $\mu_i(t)$ and $\tilde{\mu}_i(t)$, then analyze the stability of the closed-loop dynamics. Note that the desired maneuvering velocity $\dot{p}_i^*$ in (13) is a linear combination of the translation velocity v_c^*, rotation velocity $\omega^* E p_{ci}$, and scaling velocity $s(t)p_{ci}$. We first show in the following how to design μ_i and $\tilde{\mu}_i$ in (12) to achieve each maneuvering separately, then simultaneously.

1) Translation: According to (13), only considering translation maneuvering with desired v_c^*, one requires

$$v_c^* = \mu_1(t) z_{12} + \tilde{\mu}_1(t) z_{13} \tag{14}$$

$$\begin{aligned} v_c^* &= \mu_2(t) z_{23} + \tilde{\mu}_2(t) z_{21} \\ v_c^* &= \mu_3(t) z_{31} + \tilde{\mu}_3(t) z_{32} \end{aligned} \tag{15}$$

where we assume that the three agents' positions are not collinear. Then, $\mu_i(t), \tilde{\mu}_i(t), i = 1, 2, 3$ can be calculated by

$$\begin{bmatrix} \mu_i(t) \\ \tilde{\mu}_i(t) \end{bmatrix} = \begin{bmatrix} z_{i(i+1)}(1) & z_{i(i-1)}(1) \\ z_{i(i+1)}(2) & z_{i(i-1)}(2) \end{bmatrix}^{-1} \begin{bmatrix} v_c^*(1) \\ v_c^*(2) \end{bmatrix} \tag{16}$$

where $z_{i(i+1)}(1)$ and $z_{i(i+1)}(2)$ denote the first and second elements of the vector $z_{i(i+1)}$. To make (16) well-defined, the matrix $[z_{i(i+1)}\ z_{i(i-1)}]$ should always be invertible, which can be guaranteed if there is no collinearity among agents 1–3.

2) Rotation: Only considering rotation around p_c in (13), one has

$$\omega^* E p_{c1} = \mu_1(t) z_{12} + \tilde{\mu}_1(t) z_{13} \tag{17}$$

$$\omega^* E p_{c2} = \mu_2(t) z_{23} + \tilde{\mu}_2(t) z_{21} \tag{18}$$

$$\omega^* E p_{c3} = \mu_3(t) z_{31} + \tilde{\mu}_3(t) z_{32}. \tag{19}$$

Similarly, $\mu_i(t), \tilde{\mu}_i(t), i = 1, 2, 3$ can be calculated by

$$\begin{bmatrix} \mu_i(t) \\ \tilde{\mu}_i(t) \end{bmatrix} = \begin{bmatrix} z_{i(i+1)}(1) & z_{i(i-1)}(1) \\ z_{i(i+1)}(2) & z_{i(i-1)}(2) \end{bmatrix}^{-1} \begin{bmatrix} -\omega^* p_{ci}(2) \\ \omega^* p_{ci}(1) \end{bmatrix}. \tag{20}$$

3) Scaling: Only considering scaling with respect to p_c in (13), one has

$$s(t) p_{c1} = \mu_1(t) z_{12} + \tilde{\mu}_1(t) z_{13} \tag{21}$$

$$s(t) p_{c2} = \mu_2(t) z_{23} + \tilde{\mu}_2(t) z_{21} \tag{22}$$

$$s(t) p_{c3} = \mu_3(t) z_{31} + \tilde{\mu}_3(t) z_{32}. \tag{23}$$

Also, $\mu_i(t), \tilde{\mu}_i(t), i = 1, 2, 3$ can be calculated by

$$\begin{bmatrix} \mu_i(t) \\ \tilde{\mu}_i(t) \end{bmatrix} = \begin{bmatrix} z_{i(i+1)}(1) & z_{i(i-1)}(1) \\ z_{i(i+1)}(2) & z_{i(i-1)}(2) \end{bmatrix}^{-1} \begin{bmatrix} s(t) p_{ci}(1) \\ s(t) p_{ci}(2) \end{bmatrix}. \tag{24}$$

Then, by applying translation, rotation, and scaling simultaneously, one has

$$\begin{aligned} \begin{bmatrix} \mu_i(t) \\ \tilde{\mu}_i(t) \end{bmatrix} &= [z_{i(i+1)}\ z_{i(i-1)}]^{-1}(v_c^* + \omega^* E p_{ci} + s(t) p_{ci}) \\ &= [z_{i(i+1)}\ z_{i(i-1)}]^{-1} \begin{bmatrix} v_c^*(1) - \omega^* p_{ci}(2) + s(t) p_{ci}(1) \\ v_c^*(2) + \omega^* p_{ci}(1) + s(t) p_{ci}(2) \end{bmatrix} \end{aligned} \tag{25}$$

which is well defined when $[z_{i(i+1)}\ z_{i(i-1)}]$ is invertible. By applying the designed mismatches (25) into the control law (12), we are ready to give the following result.

Theorem 1: Consider a three-agent formation described by (1), with the control inputs (12) and mismatches $\mu_i(t), \tilde{\mu}_i(t), i = 1, 2, 3$ as designed in (25). If the initial angle errors $e_i(0)$ are sufficiently small, $\alpha_i(0) \neq 0$, and $\|p_i(0) - p_j(0)\|, i \neq j$ are sufficiently away from zero, then the three-agent formation converges to its desired shape and maneuvers with the combination of the prescribed translation (4), rotation (5), and scaling (6).

Proof: According to (12), the motion of each agent is influenced by the combination of formation shape control part $u_{fi} = -k_i(\alpha_i - \alpha_i^*)(z_{i(i+1)} + z_{i(i-1)})$ and maneuver control part $u_{mi} = \mu_i z_{i(i+1)} + \tilde{\mu}_i z_{i(i-1)}$. To obtain (3), we need to

analyze $\dot{e}_i$. According to Appendix A, the angle error dynamics can be described by

$$\dot{e} = \begin{bmatrix} \dot{\alpha}_1 \\ \dot{\alpha}_2 \\ \dot{\alpha}_3 \end{bmatrix} = F_1(e)e = \begin{bmatrix} -g_1 & f_{12} & f_{13} \\ f_{21} & -g_2 & f_{23} \\ f_{31} & f_{32} & -g_3 \end{bmatrix} \begin{bmatrix} e_1 \\ e_2 \\ e_3 \end{bmatrix} \tag{26}$$

where $f_{ij} := k_j(\sin\alpha_j)/l_{ij}$, $g_i := (\sin\alpha_i)(k_i/l_{i(i+1)} + k_i/l_{i(i-1)})$, and $l_{ij} := \|p_i - p_j\|$ denotes the distance between i and j. According to Appendix A and (26), the maneuver control part u_{mi} has no contribution to the angle error dynamics $\dot{e}_i$, which is reasonable since the whole formation's translation, rotation, and scaling will not change its interior angles.

First, we prove that the three-agent formation will not become collinear under (26) if it is not initially collinear. If for a fixed i, $\alpha_i \to \pi$, one has $\alpha_{i-1} \to 0$ and $\alpha_{i+1} \to 0$ because $\alpha_i + \alpha_{i-1} + \alpha_{i+1} = \pi$. Note that $\alpha_i^*, i = 1, 2, 3$ are bounded away from zero and π, which implies that $e_i > 0$, $e_{i+1} < 0$, and $e_{i-1} < 0$. Then, since $g_i > 0$ and $f_{ij} > 0, j = i-1, i+1$, from agent i's angle error dynamics $\dot{e}_i = -g_i e_i + f_{i(i+1)}e_{i+1} + f_{i(i-1)}e_{i-1}$, one has $\dot{e}_i < 0$, which implies that $\dot{\alpha}_i$ makes it impossible to achieve $\alpha_i = \pi$. Similarly should $\alpha_i \to 0$, one would obtain the contradicting result that α_i increases. Since α_i has to be 0 or π in the collinear situation, the contradictions we have constructed imply that the three agents will not become collinear if their initial positions are not collinear. Therefore, it follows that the calculations in (16)–(25) are well defined.

Since $e_1 + e_2 + e_3 \equiv 0$, the angle error dynamics (26) can be reduced to

$$\dot{e}_s = \begin{bmatrix} \dot{e}_1 \\ \dot{e}_2 \end{bmatrix} = \begin{bmatrix} -(g_1 + f_{13}) & f_{12} - f_{13} \\ f_{21} - f_{23} & -(g_2 + f_{23}) \end{bmatrix} \begin{bmatrix} e_1 \\ e_2 \end{bmatrix} = F_{s1}(e_s)e_s. \tag{27}$$

Let $\mathbb{U} \in \mathbb{R}^2$ denote the neighborhood of the origin $\{e_1 = e_2 = 0\}$, in which we investigate the local stability of (27). Linearizing (27) at the origin, we obtain

$$\dot{e}_s = A_1 e_s \tag{28}$$

where $A_1 = F_{s1}(e_s)|_{e_s=0}$. Then, under $e_s = 0$, i.e., $\alpha_i = \alpha_i^*$, one has

$$\mathrm{tr}(A_1(\alpha^*)) = -g_1 - f_{13} - g_2 - f_{23} < 0 \tag{29}$$

$$\begin{aligned} \det(A_1(\alpha^*)) &= (g_1 + f_{13})(g_2 + f_{23}) - (f_{21} - f_{23})(f_{12} - f_{13}) \\ &> g_1 f_{23} + g_2 f_{13} + f_{21} f_{13} + f_{12} f_{23} > 0 \end{aligned} \tag{30}$$

where we have used the fact that $g_1 g_2 > f_{21} f_{12}$, and tr() and det() denote the trace and determinant of a square matrix, respectively. According to (29) and (30), one has that A_1 is Hurwitz. By following the Lyapunov Theorem[24, Th. 4.6], for an arbitrary positive definite matrix $Q_1 \in \mathbb{R}^{2\times 2}$, there always exists a positive definite matrix $P_1 \in \mathbb{R}^{2\times 2}$ such that $-Q_1 = P_1 A_1 + A_1^{\mathrm{T}} P_1$. We then design the Lyapunov function candidate as $V_1 = e_s^{\mathrm{T}} P_1 e_s$, whose time derivative is

$$\dot{V}_1 = -e_s^{\mathrm{T}} Q_1 e_s \le -\left(\lambda_{\min}(Q_1)/\lambda_{\max}(P_1)\right) V_1 \tag{31}$$

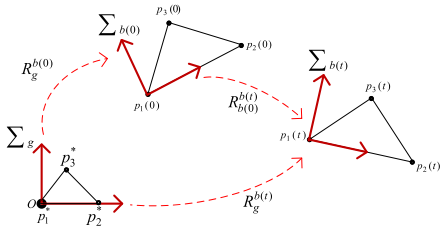

Fig. 4. Relationship between several coordinate frames.

where $\lambda_{\min}()$ and $\lambda_{\max}()$ denote the minimum and maximum eigenvalues of a square matrix, respectively. Then, one has

$$e_1^2 + e_2^2 = \|e_s\|^2 \le \frac{V_1}{\lambda_{\min}(P_1)} \le \frac{V_1(0)}{\lambda_{\min}(P_1)} e^{-\frac{\lambda_{\min}(Q_1)}{\lambda_{\max}(P_1)}t}. \tag{32}$$

Also, one has

$$e_3^2 = e_1^2 + e_2^2 + 2e_1e_2 \le 2(e_1^2 + e_2^2) \le \frac{2\,V_1(0)}{\lambda_{\min}(P_1)} e^{-\frac{\lambda_{\min}(Q_1)}{\lambda_{\max}(P_1)}t}$$

which implies that e_i under the dynamics (26) is exponentially stable when the initial states lie in $\mathbb{U}$ [24, Lemma 9.1]. Note that when $e_i(t) \to 0$, $l_{i(i+1)}(t)$ will converge to a constant since $s(t)$ in (6) can be seen as a vanishing perturbation. Using (1) and (12), one has $\lim_{t\to\infty}[\dot{p}_i(t) - (\mu_i(t) z_{i(i+1)}(t) + \tilde{\mu}_i(t) z_{i(i-1)}(t))] = 0$. Therefore, if (14)–(15), (17)–(19), or (21)–(23) are applied separately in (13), the maneuvering defined in (4)–(6) is achieved separately. Meanwhile, if they are applied simultaneously by (25), the maneuverings consisting of translation, rotation, and scaling are achieved simultaneously. ■

C. Measurement-Independent Mismatches

Now, we consider that the agent i can only measure $z_{i(i+1)}$ and $z_{i(i-1)}$ in (12). The mismatches μ_i and $\tilde{\mu}_i$ are calculated in the design stage by using the information of the desired formation shape. First, we define a body frame $\sum_{b(t)}$ whose origin is fixed at the position $p_1(t)$ of the agent 1, and x-axis points from the position $p_1(t)$ of the agent 1 to the position $p_2(t)$ of the agent 2, and y-axis follows the direction under the right-hand rule.

At the initial design stage $t = 0$, consider the static and reference formation configuration $p^{b*} = [(p_1^{b*})^{\mathrm{T}}, (p_2^{b*})^{\mathrm{T}}, \ldots, (p_N^{b*})^{\mathrm{T}}]^{\mathrm{T}} \in \mathbb{R}^{2N}$ described in $\sum_{b(0)}$, which satisfies all the desired angle constraints α^*. As shown in Fig. 4, according to the definition of $\sum_{b(0)}$, one has $p_1^{b*} = [0, 0]^{\mathrm{T}}$ and $p_2^{b*} = [x_{p_2^*}, 0]^{\mathrm{T}}$, where $x_{p_2^*}$ can be chosen as an arbitrary positive number; then, one can calculate $p_3^{b*}, \ldots, p_N^{b*}$ using the angle constraints α^*. If one has a reference configuration $p^* = [(p_1^*)^{\mathrm{T}}, (p_2^*)^{\mathrm{T}}, \ldots, (p_N^*)^{\mathrm{T}}]^{\mathrm{T}}$ of the desired formation described in $\sum_g$ with $p_1^* = [0, 0]^{\mathrm{T}}$ and $p_2^* = [x_{p_2^*}, 0]^{\mathrm{T}}$, then one directly has $p^{b*} = p^*$. Now, we use p^{b*} for the design of measurement-independent mismatches.

1) Translation: Only considering translational maneuvering, similar to (14) and (15), one has

$$v_c^{b*} = R_g^{b(0)} v_c^* = \mu_i z_{i(i+1)}^{b*} + \tilde{\mu}_i z_{i(i-1)}^{b*}, i = 1, 2, 3 \tag{33}$$

where $z_{ij}^{b*}=\frac{p_j^{b*}-p_i^{b*}}{\|p_j^{b*}-p_i^{b*}\|}$ is the bearing calculated by p^{b*}, v_c^* is described in $\sum_g$, and $R_g^{b(0)}$ is the rotation matrix from $\sum_g$ to $\sum_{b(0)}$. Then, $\mu_i,\tilde{\mu}_i, i=1,2,3$ can be calculated by

$$\begin{bmatrix}\mu_i\\ \tilde{\mu}_i\end{bmatrix}=\begin{bmatrix}z_{i(i+1)}^{b*}(1) & z_{i(i-1)}^{b*}(1)\\ z_{i(i+1)}^{b*}(2) & z_{i(i-1)}^{b*}(2)\end{bmatrix}^{-1}\begin{bmatrix}v_c^{b*}(1)\\ v_c^{b*}(2)\end{bmatrix}. \tag{34}$$

Since the bearing vectors $z_{i(i+1)}^{b*}$ and $z_{i(i-1)}^{b*}$ are noncollinear in a generically angle rigid formation according to [20, Definition 4] and Assumption 1, the matrix $[z_{i(i+1)}^{b*}\ z_{i(i-1)}^{b*}]$ is invertible. Since v_c^{b*} is described in $\sum_{b(0)}$ in (33), the control objective (4) for translation maneuvering in this case should be modified to

$$\lim_{t\to\infty}(R_g^{b(t)}\dot{p}_i(t)-v_c^{b*})=0 \tag{35}$$

where $R_g^{b(t)}$ is the rotation matrix from $\sum_g$ to $\sum_{b(t)}$.

2) Rotation: Considering rotation in (13), one has

$$\omega^* E p_{ci}^{b*}=\mu_i z_{i(i+1)}^{b*}+\tilde{\mu}_i z_{i(i-1)}^{b*}, i=1,2,3 \tag{36}$$

where $p_{ci}^{b*}=p_i^{b*}-p_c^{b*}=p_i^{b*}-\frac{1}{N}\sum_{j=1}^N p_j^{b*}$. Then, $\mu_i,\tilde{\mu}_i, i=1,2,3$ can be similarly calculated as (24).

3) Scaling: Only considering scaling with respect to the p_c^{b*} in (13), one has

$$s(t)p_{ci}^{b*}=\mu_i z_{i(i+1)}^{b*}+\tilde{\mu}_i z_{i(i-1)}^{b*}. \tag{37}$$

Then, $\mu_i,\tilde{\mu}_i, i=1,2,3$ can be calculated. Then, by applying translation, rotation, and scaling simultaneously, one has

$$\begin{bmatrix}\mu_i\\ \tilde{\mu}_i\end{bmatrix}=[z_{i(i+1)}^{b*}\ z_{i(i-1)}^{b*}]^{-1}\left(v_c^{b*}+\omega^* E p_{ci}^{b*}+s(t)p_{ci}^{b*}\right) \tag{38}$$

which is well-defined since $[z_{i(i+1)}^{b*}\ z_{i(i-1)}^{b*}]\in\mathbb{R}^{2\times 2}$ is invertible. Now, we apply the constant mismatches designed in (38) into the control law (12).

Theorem 2: Consider a three-agent formation described by (1), with the control inputs (12) and mismatches $\mu_i,\tilde{\mu}_i, i=1,2,3$ as designed in (38). If the initial angle error $e_i(0)$, and the designed mismatches are sufficiently small, $\alpha_i(0)\neq 0$ and $\|p_i(0)-p_j(0)\|, i\neq j$ are sufficiently away from zero, then the three-agent formation converges to its desired shape and maneuvers with the prescribed translation (35), rotation (5), and scaling (6).

Proof: To analyze the convergence of e_i, we first aim at obtaining the angle error dynamics $\dot{e}_i, i=1,2,3$. Note that the analysis method of angle error dynamics given in [21] cannot be used in this case because of the part $\mu_i z_{i(i+1)}+\tilde{\mu}_i z_{i(i-1)}$ in the control law (12). Instead, we derive the angle error dynamics by using the dot product of two bearings. Using similar steps as Appendix A, one has the following angle error dynamics under the control (12) and (38):

$$\begin{aligned}\dot{e}&=[\dot{\alpha}_1\ \dot{\alpha}_2\ \dot{\alpha}_3]^{\mathrm{T}}=F_2(e)e+H_2(e,\mu,\tilde{\mu})\\ &=\begin{bmatrix}-g_1 & f_{12} & f_{13}\\ f_{21} & -g_2 & f_{23}\\ f_{31} & f_{32} & -g_3\end{bmatrix}\begin{bmatrix}\alpha_1-\alpha_1^*\\ \alpha_2-\alpha_2^*\\ \alpha_3-\alpha_3^*\end{bmatrix}+\begin{bmatrix}h_1\\ h_2\\ h_3\end{bmatrix}\end{aligned} \tag{39}$$

where g_i and f_{ij} have the same forms as (26), and

$$h_i=\frac{\tilde{\mu}_i\sin\alpha_i-\mu_{i+1}\sin\alpha_{i+1}}{l_{i(i+1)}}+\frac{\mu_i\sin\alpha_i-\tilde{\mu}_{i-1}\sin\alpha_{i-1}}{l_{i(i-1)}}.$$

Now, we analyze the local stability of (39). Since $e_1+e_2+e_3=0$, one has the following subdynamics:

$$\begin{aligned}\dot{e}_s&=\begin{bmatrix}\dot{e}_1\\ \dot{e}_2\end{bmatrix}=F_{s2}(e_s)e_s+H_{s2}(e_s)U_2\\ &=\begin{bmatrix}-(g_1+f_{13}) & f_{12}-f_{13}\\ f_{21}-f_{23} & -(g_2+f_{23})\end{bmatrix}\begin{bmatrix}\alpha_1-\alpha_1^*\\ \alpha_2-\alpha_2^*\end{bmatrix}\\ &\quad+\begin{bmatrix}h_{11} & h_{12} & h_{13} & h_{14} & h_{15} & h_{16}\\ h_{21} & h_{22} & h_{23} & h_{24} & h_{25} & h_{26}\end{bmatrix}U_2\end{aligned} \tag{40}$$

where $U_2=[\mu_1,\mu_2,\mu_3,\tilde{\mu}_1,\tilde{\mu}_2,\tilde{\mu}_3]^{\mathrm{T}}$, $h_{11}=\frac{\sin\alpha_1}{l_{13}}$, $h_{12}=-\frac{\sin\alpha_2}{l_{12}}$, $h_{13}=h_{15}=0$, $h_{14}=\frac{\sin\alpha_1}{l_{12}}$, $h_{16}=-\frac{\sin\alpha_3}{l_{13}}$, $h_{21}=h_{26}=0$, $h_{22}=\frac{\sin\alpha_2}{l_{21}}$, $h_{23}=-\frac{\sin\alpha_3}{l_{23}}$, $h_{24}=-\frac{\sin\alpha_1}{l_{21}}$, and $h_{25}=-\frac{\sin\alpha_2}{l_{23}}$. It can be verified that $H_2(0,\mu,\tilde{\mu})=0$, which implies that $e=0$ is an equilibrium of (39). To obtain the local stability of (40), we linearize the dynamics (40) at the origin. The linearized system of (40) at the origin can be written as

$$\dot{e}_s=A_1e_s+B_1e_s=(A_1+B_1)e_s$$

where $B_1=\frac{\partial H_{s2}(e_s)U_2}{\partial e_s}|_{e_s=0}=[\frac{\partial H_{s2}(e_s)}{\partial e_1}\ \frac{\partial H_{s2}(e_s)}{\partial e_2}](I_2\otimes U_2)|_{e_s=0}$, and $A_1=F_{s2}(e_s)|_{e_s=0}$, $\otimes$ and I_N denote the Kronecker product and N-by-N identity matrix, respectively. Therefore, for an arbitrary positive definite matrix $Q_2\in\mathbb{R}^{2\times 2}$, there exists a positive definite matrix $P_2\in\mathbb{R}^{2\times 2}$ such that $Q_2=-(P_2A_1+A_1^{\mathrm{T}}P_2)$. Since U_2 is bounded, we then check the stability of (40) when e_s lies in $\mathbb{U}$. Consider the Lyapunov function candidate $V_2=e_s^{\mathrm{T}}P_2e_s$ whose time derivative is

$$\begin{aligned}\dot{V}_2&\le-\lambda_{\min}(Q_2)\|e_s\|^2+e_s^{\mathrm{T}}(B_1^{\mathrm{T}}P_2+P_2B_1)e_s\\ &\le(-\lambda_{\min}(Q_2)+q_1)\|e_s\|^2\end{aligned} \tag{41}$$

where $q_1=2\|B_1\|\lambda_{\max}(P_2)$. For a neighborhood of the equilibrium, one can obtain $\lambda_{\min}(Q_2)>q_1$ by choosing the following:

1) *Small designed-mismatches* $\mu_i,\tilde{\mu}_i$: since $q_1(\mu)$ grows with μ continuously and $q_1(\mu)\ge q_1(0)=0$, which in general require that the maneuvering speed $\|v_c^*\|,\omega^*,k_s$ should be sufficiently small according to (38);
2) *Big feedback gain* k_i *when* $k_1=k_2=k_3$: which only makes $\lambda_{\max}(P_2)$ smaller but not $\lambda_{\min}(Q_2)$ because Q_2 is given and $\|B_1\|$ is not related with k_i.

When $\lambda_{\min}(Q_2)>q_1$, the subdynamics (40) are locally exponentially stable. By following (31) and (32), one has

$$e_1^2+e_2^2=\|e_s\|^2\le\frac{V_2}{\lambda_{\min}(P_2)}\le\frac{V_2(0)}{\lambda_{\min}(P_2)}e^{-\frac{\lambda_{\min}(Q_2)-q_1}{\lambda_{\max}(P_2)}t}. \tag{42}$$

Since $e_1=e_2=0$ implies $e_3=0$, the overall dynamics (39) are locally exponentially stable, which implies that $\lim_{t\to\infty}[\dot{p}_i(t)-(\mu_i z_{i(i+1)}(t)+\tilde{\mu}_i z_{i(i-1)}(t))]=0$. For the translation case, it follows that $\lim_{t\to\infty}R_g^{b(t)}\dot{p}_i(t)=\lim_{t\to\infty}R_g^{b(t)}(\mu_i z_{i(i+1)}(t)+$

$\tilde{\mu}_i z_{i(i-1)}(t)) = \lim_{t\to\infty}(\mu_i z^{b(t)}_{i(i+1)}(t) + \tilde{\mu}_i z^{b(t)}_{i(i-1)}(t)) = v_c^{b*}$, where we have used the facts that $\sum_{b(t)}$ is rigidly attached at the real-time formation and $z^{b(t)}_{ij}(t) \to z^{b*}_{ij}$ when $\alpha_i \to \alpha_i^*$. For rotation and scaling, since $k_s p^{b*}_{ci} = \mu_i z^{b*}_{i(i+1)} + \tilde{\mu}_i z^{b*}_{i(i-1)}$ implies that $k_s p_{ci} = \mu_i z_{i(i+1)} + \tilde{\mu}_i z_{i(i-1)}$, one has that the rotation and scaling are also achieved. Therefore, the maneuvering defined in (5), (6), and (35) is achieved. Note that the formation's eventual orientation $R^g_{b(\infty)}$ is not necessarily equal to $R^g_{b(0)}$. The eventual maneuvering velocity described in $\sum_g$ is $\lim_{t\to\infty}\dot{p}_i(t) = R^g_{b(\infty)} v_c^{b*} + \omega^* E p_{ci}(\infty) + k_s p_{ci}(\infty)$ where the formation's eventual orientation $R^g_{b(\infty)}$ depends on the initial states of the agents and the rotation maneuvering that the formation has conducted. Finally, we analyze the noncollinearity in this case. Note that (42) implies that $\forall i = 1, 2, 3$

$$|e_i| = |\alpha_i - \alpha_i^*| \le \sqrt{\frac{2\,V_2(0)}{\lambda_{\min}(P_2)}} e^{-\frac{\lambda_{\min}(Q_2)-q_1}{2\lambda_{\max}(P_2)}t} \le \sqrt{\frac{2\,V_2(0)}{\lambda_{\min}(P_2)}}.$$

If we choose the initial formation errors $e_i(0)$ such that $V_2(0)$ is sufficiently small, one has that $\alpha_i(t)$ will be bounded away from zero and π because $\alpha_i^*, i = 1, 2, 3$ are bounded away from zero and π. This implies that no collinearity will occur in this case. ■

Remark 2: For the case of measurement-independent mismatches, (12) can be realized in each agent's local coordinate frame that can have different orientation from $\sum_g$. Note that the measurement-independent mismatches in (38) can be calculated in the design stage that uses the information of the desired formation shape p^{b*} described in $\sum_{b(0)}$. However, the implementation of (12) is distributed, i.e., no aligned coordinate frames or global information is required to be shared among agents.

Remark 3: Note that the desired translation velocity in (14) and (15) is described in $\sum_g$, but in (33), it is described in $\sum_{b(0)}$. To achieve a desired translational velocity with respect to $\sum_g$ in the measurement-independent mismatch case, one can align one real-time bearing z_{ij} to the bearing z^{b*}_{ij} described in $\sum_{b(0)}$[10]. However, the mismatch design for rotation and scaling in both measurement-dependent and measurement-independent cases is not influenced by the global or local coordinate frame because the rotation and scaling is conducted with respect to the formation's reference point p_c instead of an external reference frame; see Fig. 2 and (4)–(6).

Remark 4: For the case of measurement-dependent mismatches, one can also add the desired maneuvering velocity $v_c^* + \omega^* E p_{ci} + s(t) p_{ci}$ directly into (11). The reasons for designing measurement-dependent mismatches are supported by two facts. The first is that the controllers for the cases of measurement-dependent and measurement-independent mismatches have the same form (12). Therefore, when the measurements of relative position are available, the formation maneuvering can be realized with measurement-dependent mismatches, but when they are unavailable, the formation maneuvering can be realized with measurement-independent mismatches whose control law has the same structure as the measurement-dependent case. The second is that the analysis of angle error dynamics (39) in the case of measurement-independent mismatches is based on the angle error dynamics (26) in the case of measurement-dependent mismatches.

D. Collision Analysis

Note that the angle error dynamics and the bearing vector $z_{ij} = \frac{p_j - p_i}{\|p_j - p_i\|}, j \in \mathcal{N}_i$ used in the maneuver control law (12) are not well defined if there exists collision between neighboring agents i and j. Therefore, the analysis on the collision among the three agents is needed. Since we are controlling interior angles, we would like to show that the distance $l_{ij} = \|p_i - p_j\|$ does not vary much, which is not obvious when maneuvering is conducted. Therefore, we need to assess the order of magnitude of how much l_{ij} can grow or shrink from the initial conditions. Consequently, we provide the following analysis considering the cases of measurement-dependent and measurement-independent mismatches, respectively.

1) Measurement-Dependent Mismatches: Taking agents 1 and 2 as an example (the other cases can be similarly analyzed), one has

$$\begin{aligned} l_{12}(t) &= l_{12}(0) + \int_0^t \dot{l}_{12}(\tau)\mathrm{d}\tau \\ &= l_{12}(0) + \int_0^t \frac{(p_1 - p_2)^{\mathrm{T}}(\dot{p}_1 - \dot{p}_2)}{\|p_1 - p_2\|}\mathrm{d}\tau \\ &= l_{12}(0) + \int_0^t z_{21}^{\mathrm{T}}(u_{f1} - u_{f2} + u_{m1} - u_{m2})\mathrm{d}\tau. \end{aligned} \quad (43)$$

First, we consider the formation part $u_{f1} - u_{f2}$ in (43)

$$\begin{aligned} &\int_0^t z_{21}^{\mathrm{T}}(u_{f1} - u_{f2})\mathrm{d}\tau \\ &= \int_0^t k_2 e_2 z_{21}^{\mathrm{T}}(z_{21} + z_{23}) - k_1 e_1 z_{21}^{\mathrm{T}}(z_{12} + z_{13})\mathrm{d}\tau \\ &\le \int_0^t (2k_1|e_1| + 2k_2|e_2|)\mathrm{d}\tau \le 2\sqrt{2}\bar{k}_{12}\int_0^t \sqrt{e_1^2 + e_2^2}\mathrm{d}\tau \end{aligned} \quad (44)$$

where $\bar{k}_{12} = \max\{k_1, k_2\}$ and we have used the fact that $2|e_1||e_2| \le e_1^2 + e_2^2$. By using (32), one has

$$\begin{aligned} \int_0^t \sqrt{e_1^2 + e_2^2}\mathrm{d}\tau &\le \sqrt{\frac{V_1(0)}{\lambda_{\min}(P_1)}}\frac{2\lambda_{\max}(P_1)}{\lambda_{\min}(Q_1)}\left(1 - e^{-\frac{\lambda_{\min}(Q_1)}{2\lambda_{\max}(P_1)}t}\right) \\ &\le \frac{2\lambda_{\max}(P_1)}{\lambda_{\min}(Q_1)}\sqrt{\frac{V_1(0)}{\lambda_{\min}(P_1)}}. \end{aligned} \quad (45)$$

Then, we consider the maneuver part $u_{m1} - u_{m2}$ in (43). By using (12) and (25), one has

$$\begin{aligned} \int_0^t z_{21}^{\mathrm{T}}(u_{m1} - u_{m2})\mathrm{d}\tau &= \int_0^t z_{21}^{\mathrm{T}}[\omega^* E + s(\tau) I_2](p_{c1} - p_{c2})\mathrm{d}\tau \\ &= \int_0^t s(\tau) l_{12}(\tau)\mathrm{d}\tau \end{aligned} \quad (46)$$

where we have used the fact that $z_{21}^{\mathrm{T}}Ez_{21}=0$ and $p_{c1}-p_{c2}=z_{21}l_{12}$. According to (46), the translational and rotational maneuvering has no impact on the change of $l_{12}(t)$, and only scaling has. Note that when modulation factor for the scaling speed $s(t)>0$, i.e., conducting formation enlargement, one always has $\int_0^t s(\tau)l_{12}(\tau)\mathrm{d}\tau\geq 0$. By substituting (44)–(46) into (43), when $s(t)>0$, one has

$$l_{12}(t)\geq l_{12}(0)+\int_0^t s(\tau)l_{12}(\tau)\mathrm{d}\tau-\frac{4\bar{k}_{12}\lambda_{\max}(P_1)}{\lambda_{\min}(Q_1)}\sqrt{\frac{2V_1(0)}{\lambda_{\min}(P_1)}}$$
$$\geq l_{12}(0)-\frac{4\bar{k}_{12}\lambda_{\max}(P_1)}{\lambda_{\min}(Q_1)}\sqrt{\frac{2V_1(0)}{\lambda_{\min}(P_1)}}. \tag{47}$$

However, the case of $s(t)<0$ is also important in the obstacle avoidance task because it corresponds to shrink the formation. Now, we analyze the impact of shrinking formation on the change of $l_{12}(t)$ using the case $k_s=-1$. By using the integration by parts, one has

$$\int_0^t s(\tau)l_{12}(\tau)\mathrm{d}\tau=\gamma^{-1}l_{12}e^{-\gamma t}-\gamma^{-1}\int_0^t e^{-\gamma\tau}\mathrm{d}l_{12}(\tau)$$
$$=\gamma^{-1}l_{12}e^{-\gamma t}-\gamma^{-1}\int_0^t e^{-\gamma\tau}s(\tau)l_{12}(\tau)\mathrm{d}\tau$$
$$-\gamma^{-1}\int_0^t e^{-\gamma\tau}[z_{21}^{\mathrm{T}}(u_{f1}-u_{f2})]\mathrm{d}\tau. \tag{48}$$

Note that in (48), $\gamma^{-1}l_{12}e^{-\gamma t}\geq 0$ and $-\gamma^{-1}\int_0^t e^{-\gamma\tau}s(\tau)l_{12}(\tau)\mathrm{d}\tau\geq 0$ since $s(t)<0$. In addition, by using (44), one has

$$-\gamma^{-1}\int_0^t e^{-\gamma\tau}[z_{21}^{\mathrm{T}}(u_{f1}-u_{f2})]\mathrm{d}\tau$$
$$\leq\gamma^{-1}2\sqrt{2}\bar{k}_{12}\int_0^t e^{-\gamma\tau}\sqrt{e_1^2+e_2^2}\,\mathrm{d}\tau$$
$$\leq\gamma^{-1}2\sqrt{2}\bar{k}_{12}\sqrt{\frac{V_1(0)}{\lambda_{\min}(P_1)}}\int_0^t e^{-(\gamma+\frac{\lambda_{\min}(Q_1)}{2\lambda_{\max}(P_1)})\tau}\mathrm{d}\tau$$
$$\leq\gamma^{-1}2\sqrt{2}\bar{k}_{12}\sqrt{\frac{V_1(0)}{\lambda_{\min}(P_1)}}\frac{2\lambda_{\max}(P_1)}{\lambda_{\min}(Q_1)+2\gamma\lambda_{\max}(P_1)}. \tag{49}$$

By substituting (44)–(52) into (43), when $s(t)=-e^{-\gamma t}$, one has

$$l_{12}(t)\geq l_{12}(0)-\frac{4\bar{k}_{12}\lambda_{\max}(P_1)}{\lambda_{\min}(Q_1)}\sqrt{\frac{2V_1(0)}{\lambda_{\min}(P_1)}}$$
$$-\gamma^{-1}2\sqrt{2}\bar{k}_{12}\sqrt{\frac{V_1(0)}{\lambda_{\min}(P_1)}}\frac{2\lambda_{\max}(P_1)}{\lambda_{\min}(Q_1)+2\gamma\lambda_{\max}(P_1)}. \tag{50}$$

Finally, we summarize the aforementioned analysis into a proposition.

Proposition 1: Consider a three-agent formation described by (1), with the control input (12) and mismatches $\mu_i(t),\tilde{\mu}_i(t),i=1,2,3$ as designed in (25) and $\alpha_i(0)\neq 0$. For the case of $s(t)>0$, if $l_{12}(0)>\frac{4\bar{k}_{12}\lambda_{\max}(P_1)}{\lambda_{\min}(Q_1)}\sqrt{\frac{2V_1(0)}{\lambda_{\min}(P_1)}}$, no collision will happen between agents 1 and 2. For the case of $s(t)=-e^{-\gamma t}<0$, if $l_{12}(0)>\frac{4\bar{k}_{12}\lambda_{\max}(P_1)}{\lambda_{\min}(Q_1)}\sqrt{\frac{2V_1(0)}{\lambda_{\min}(P_1)}}+\gamma^{-1}2\sqrt{2}\bar{k}_{12}\sqrt{\frac{V_1(0)}{\lambda_{\min}(P_1)}}\frac{2\lambda_{\max}(P_1)}{\lambda_{\min}(Q_1)+2\gamma\lambda_{\max}(P_1)}$, then no collision will happen between agents 1 and 2.

Proof: For the case of $s(t)>0$, since $l_{12}(0)>0$, $\exists T_2>0$ such that in $[0,T_2)$, no collision happens between agents 1 and 2. Assume that there exists a collision between agents 1 and 2 in $[T_2,\infty)$, then there must exist an escape time T_c such that $l_{12}(T_c)=0$. Since no collision happens in $[T_2,T_c^-)$, the closed-loop system is well defined in $[T_2,T_c^-)$. Following the calculations in (43)–(47), one has that $l_{12}(T_c^-)\geq l_{12}(0)-\frac{4\bar{k}_{12}\lambda_{\max}(P_1)}{\lambda_{\min}(Q_1)}\sqrt{\frac{2V_1(0)}{\lambda_{\min}(P_1)}}>0$, which is bounded away from zero. This implies a contradiction with the assumption that collision happens at T_c. Thus, no collision happens in $[0,\infty)$. The case of $s(t)<0$ can be similarly obtained. ■

2) Measurement-Independent Mismatches: For the case of measurement-independent mismatches, the description of $l_{12}(t)$ in (43) still holds. By following the analysis from (43) to (45), one has the effect of the formation part $u_{f1}-u_{f2}$ on $l_{21}(t)$

$$\int_0^t z_{21}^{\mathrm{T}}(u_{f1}-u_{f2})\mathrm{d}\tau\leq 2\sqrt{2}\bar{k}_{12}\int_0^t\sqrt{e_1^2+e_2^2}\mathrm{d}\tau$$
$$\leq\frac{4\bar{k}_{12}\lambda_{\max}(P_2)}{\lambda_{\min}(Q_2)-q_1}\sqrt{\frac{2V_2(0)}{\lambda_{\min}(P_2)}}. \tag{51}$$

Then, we discuss the maneuver part $u_{m1}-u_{m2}$ in (43). By using (12) and (38), one has

$$\int_0^t z_{21}^{\mathrm{T}}(u_{m1}-u_{m2})\mathrm{d}\tau$$
$$=\int_0^t z_{21}^{\mathrm{T}}(\mu_1 z_{12}+\tilde{\mu}_1 z_{13}-\mu_2 z_{23}-\tilde{\mu}_2 z_{21})\mathrm{d}\tau$$
$$=\int_0^t(-\mu_1-\tilde{\mu}_2-\tilde{\mu}_1\cos\alpha_1-\mu_2\cos\alpha_2)\mathrm{d}\tau. \tag{52}$$

By using $\alpha_i=e_i+\alpha_i^*$, one has

$$-\mu_1-\tilde{\mu}_2-\tilde{\mu}_1\cos\alpha_1-\mu_2\cos\alpha_2$$
$$=-\mu_1-\tilde{\mu}_2-\tilde{\mu}_1(\cos e_1\cos\alpha_1^*-\sin e_1\sin\alpha_1^*)$$
$$-\mu_2(\cos e_2\cos\alpha_2^*-\sin e_2\sin\alpha_2^*). \tag{53}$$

Now, we use the Taylor series to describe $\cos e_i$ and $\sin e_i$

$$\cos e_i=1-\frac{e_i^2}{2!}+\frac{e_i^4}{4!}+\cdots+\frac{(-1)^n e_i^{2n}}{(2n)!} \tag{54}$$

$$\sin e_i=e_i-\frac{e_i^3}{3!}+\frac{e_i^5}{5!}+\cdots+\frac{(-1)^n e_i^{2n+1}}{(2n+1)!} \tag{55}$$

where $n\to\infty$ and $n!$ denotes the factorial of n. Since $e_i(0)$ is sufficiently small and $e_i(t)$ converges to zero at an exponential speed, we only focus on the first main part in (54) and (55).

Then, one has

$$\begin{aligned}&-\mu_1-\tilde{\mu}_2-\tilde{\mu}_1\cos\alpha_1-\mu_2\cos\alpha_2\\&\approx-\mu_1-\tilde{\mu}_1\cos\alpha_1^*-\tilde{\mu}_2-\mu_2\cos\alpha_2^*\\&\quad+\tilde{\mu}_1e_1\sin\alpha_1^*+\mu_2e_2\sin\alpha_2^*.\end{aligned}\tag{56}$$

On the one hand, by using (38) for the first part of (56), one has

$$\begin{aligned}&-\mu_1-\tilde{\mu}_1\cos\alpha_1^*-\tilde{\mu}_2-\mu_2\cos\alpha_2^*\\&=-\begin{bmatrix}1&(z_{12}^{b*})^Tz_{13}^{b*}\end{bmatrix}\begin{bmatrix}\mu_1\\\tilde{\mu}_1\end{bmatrix}-\begin{bmatrix}(z_{21}^{b*})^\top z_{23}^*&1\end{bmatrix}\begin{bmatrix}\mu_2\\\tilde{\mu}_2\end{bmatrix}\\&=-(z_{12}^{b*})^\top\begin{bmatrix}z_{12}^{b*}&z_{13}^{b*}\end{bmatrix}[z_{12}^{b*}\,z_{13}^{b*}]^{-1}\left(v_c^{b*}+\omega^*Ep_{c1}^{b*}+s(t)p_{c1}^{b*}\right)\\&\quad-(z_{21}^{b*})^\top\begin{bmatrix}z_{23}^{b*}&z_{21}^{b*}\end{bmatrix}[z_{23}^{b*}\,z_{21}^{b*}]^{-1}\left(v_c^{b*}+\omega^*Ep_{c2}^{b*}+s(t)p_{c2}^{b*}\right)\\&=(z_{12}^{b*})^\top[\omega^*E(p_2^{b*}-p_1^{b*})+s(t)(p_2^{b*}-p_1^{b*})]=s(t)l_{12}^{b*}\end{aligned}\tag{57}$$

where we have used the fact that $\cos\alpha_1^*=(z_{12}^{b*})^{\mathrm{T}}z_{13}^{b*}$. On the other hand, for the second part of (56), one has

$$\int_0^t(\tilde{\mu}_1e_1\sin\alpha_1^*+\mu_2e_2\sin\alpha_2^*)\mathrm{d}\tau\le\int_0^t\mu_{\max 12}(|e_1|+|e_2|)\mathrm{d}\tau$$

where $\mu_{\max 12}=\max\{|\tilde{\mu}_1|,|\mu_2|\}$ and we have used the fact that $|\sin\alpha_i^*|<1$. By following (44) and (45), one has

$$\begin{aligned}\int_0^t(|e_1|+|e_2|)\mathrm{d}\tau&\le\sqrt{2}\int_0^t\sqrt{e_1^2+e_2^2}\mathrm{d}\tau\\&\le\frac{2\lambda_{\max}(P_2)}{\lambda_{\min}(Q_2)-q_1}\sqrt{\frac{2\,V_2(0)}{\lambda_{\min}(P_2)}}.\end{aligned}\tag{58}$$

By substituting (51)–(58), one has

$$\begin{aligned}l_{12}(t)\ge l_{12}(0)+\int_0^t s(t)l_{12}^{b*}\mathrm{d}\tau-\frac{4\bar{k}_{12}\lambda_{\max}(P_2)}{\lambda_{\min}(Q_2)-q_1}\sqrt{\frac{2\,V_2(0)}{\lambda_{\min}(P_2)}}\\-\frac{2\mu_{\max 12}\lambda_{\max}(P_2)}{\lambda_{\min}(Q_2)-q_1}\sqrt{\frac{2\,V_2(0)}{\lambda_{\min}(P_2)}}\end{aligned}\tag{59}$$

where $\int_0^t s(t)l_{12}^{b*}\mathrm{d}\tau>0$ when $k_s>0$. For the case of $k_s<0$, the conclusion can be similarly analyzed by following (48) and (49). Finally, we summarize the aforementioned analysis into a proposition.

Proposition 2: Consider the three-agent formation described by (1), with the control inputs (12) and mismatches $\mu_i,\tilde{\mu}_i,i=1,2,3$ as designed in (38), and the initial angle error $e_i(0)$, and the designed-mismatches are sufficiently small, $\alpha_i(0)\neq 0$ and $k_s>0$. If $l_{12}(0)>\frac{4\bar{k}_{12}\lambda_{\max}(P_2)}{\lambda_{\min}(Q_2)-q_1}\sqrt{\frac{2\,V_2(0)}{\lambda_{\min}(P_2)}}+\frac{2\mu_{\max 12}\lambda_{\max}(P_2)}{\lambda_{\min}(Q_2)-q_1}\sqrt{\frac{2\,V_2(0)}{\lambda_{\min}(P_2)}}$, then no collision will happen between agents 1 and 2.

The proof can be similarly obtained by following Proposition 1.

IV. Extension to Generically Angle Rigid Formations

In this section, we aim at realizing N-agent formation maneuver control by using designed mismatches. Since the maneuvering for the first three agents is realized, we now consider how agent $i,i=4,\ldots,N$ can be added to the formation by giving two desired angles $\alpha_{j_1ij_2}^*$ and $\alpha_{j_2ij_3}^*,j_1<i,j_2<i,j_3<i$. As shown in Fig. 3, we first investigate how the agent 4 can be merged with the first triangular formation, and then, we illustrate how agents 5 to N can be similarly merged into the resulting formations.

We can design a similar stabilization control algorithm for the agent 4 to achieve the two desired angles α_{142}^* and α_{243}^*

$$\begin{aligned}u_4=&-k_{41}(\alpha_{142}-\alpha_{142}^*)(z_{41}+z_{42})\\&-k_{42}(\alpha_{243}-\alpha_{243}^*)(z_{42}+z_{43})\end{aligned}\tag{60}$$

where k_{41} and k_{42} are positive constants. To make agent 4 also maneuver with the desired translation, rotation, and scaling, we modify the stabilization control algorithm (60) as the following formation maneuver control algorithm:

$$\begin{aligned}u_4=&-k_{41}\left(\alpha_{142}-\alpha_{142}^*-\frac{\mu_4}{k_{41}}\right)(z_{41}+z_{42})\\&-k_{42}\left(\alpha_{243}-\alpha_{243}^*-\frac{\tilde{\mu}_4}{k_{42}}\right)(z_{42}+z_{43})\\=&-k_{41}(\alpha_{142}-\alpha_{142}^*)(z_{41}+z_{42})-k_{42}(\alpha_{243}-\alpha_{243}^*)(z_{42}\\&+z_{43})+\mu_4z_{41}+(\mu_4+\tilde{\mu}_4)z_{42}+\tilde{\mu}_4z_{43}\\=&\,u_{f4}+u_{m4}\end{aligned}\tag{61}$$

where $\mu_4\in\mathbb{R}$ and $\tilde{\mu}_4\in\mathbb{R}$ are the designed-mismatches associated with agent 4's desired angles α_{142}^* and α_{243}^*. By following the similar steps given in Sections III- B and III-C, we give the following procedure for the measurement-dependent and measurement-independent mismatch design, respectively.

A. Measurement-Dependent Mismatches

Similar to the design procedure (14)–(25), we use the mismatches $\mu_4(t),\tilde{\mu}_4(t)$ to realize the desired maneuvering under the measurements of $z_{4i},i=1,2,3$ and $p_{c4}=p_4-p_c$.

1) Translation: According to (13), only considering translation maneuvering, one requires

$$v_c^*=\mu_4(t)z_{41}+(\mu_4(t)+\tilde{\mu}_4(t))z_{42}+\tilde{\mu}_4(t)z_{43}.\tag{62}$$

Then, $\mu_4(t)$ and $\tilde{\mu}_4(t)$ can be calculated by

$$\begin{bmatrix}\mu_4(t)\\\tilde{\mu}_4(t)\end{bmatrix}=\begin{bmatrix}(z_{41}+z_{42})(1)&(z_{42}+z_{43})(1)\\(z_{41}+z_{42})(2)&(z_{42}+z_{43})(2)\end{bmatrix}^{-1}\begin{bmatrix}v_c^*(1)\\v_c^*(2)\end{bmatrix}.$$

2) Rotation: Based on (13), considering rotation maneuvering, one has

$$\omega^*Ep_{c4}=\mu_4(t)z_{41}+(\mu_4(t)+\tilde{\mu}_4(t))z_{42}+\tilde{\mu}_4(t)z_{43}.\tag{63}$$

Similarly, $\mu_4(t)$ and $\tilde{\mu}_4(t)$ can be calculated.

3) Scaling: Only considering scaling maneuvering in (13), one has

$$s(t)p_{c4} = \mu_4(t)z_{41} + (\mu_4(t) + \tilde{\mu}_4(t))z_{42} + \tilde{\mu}_4(t)z_{43}. \quad (64)$$

Then, $\mu_4(t)$ and $\tilde{\mu}_4(t)$ can be calculated. By applying translation, rotation, and scaling simultaneously, one has

$$\begin{bmatrix}\mu_4(t)\\ \tilde{\mu}_4(t)\end{bmatrix} = [z_{41}+z_{42} \quad z_{42}+z_{43}]^{-1}(v_c^* + \omega^* E p_{c4} + s(t)p_{c4}). \quad (65)$$

Now, we give the result for the four-agent case.

Theorem 3: Consider a four-agent formation described by (1), with the control (12) for agents 1 to 3, the control (61) for the agent 4, and the mismatches $\mu_i(t), \tilde{\mu}_i(t), i = 1, 2, 3$ as designed in (25), and $\mu_4, \tilde{\mu}_4$ as designed in (65). If the initial angle errors $e_i(0), i = 1, 2, 3$ and $e_{41}(0), e_{42}(0)$ are sufficiently small, $\alpha_i(0) \neq 0, \sin\alpha_{124}^* > \sin\alpha_{214}^*, \sin\alpha_{423}^* > \sin\alpha_{234}^*$, and $\alpha_{143}^* = \alpha_{142}^* + \alpha_{243}^*$ and $\|p_i(0) - p_j(0)\|, i \neq j$ are sufficiently away from zero, then the four-agent formation converges to its desired shape and maneuvers with the prescribed translation, rotation, and scaling.

Proof: According to Appendix B, one has agent 4's angle error dynamics

$$\dot{e}_4 = \begin{bmatrix}\dot{e}_{41}\\ \dot{e}_{42}\end{bmatrix} = F_4(e_4)e_4 + W(e_4)e_s$$
$$= \begin{bmatrix}-\bar{g}_1 & \bar{f}_{12}\\ \bar{f}_{21} & -\bar{g}_2\end{bmatrix}\begin{bmatrix}\alpha_{142}-\alpha_{142}^*\\ \alpha_{243}-\alpha_{243}^*\end{bmatrix} + \begin{bmatrix}w_{11} & w_{12}\\ w_{21} & w_{22}\end{bmatrix}\begin{bmatrix}e_1\\ e_2\end{bmatrix} \quad (66)$$

where $\bar{g}_1 = k_{41}\sin\alpha_{142}(1/l_{41} + 1/l_{42})$, $\bar{g}_2 = k_{42}\sin\alpha_{243}(1/l_{43}+1/l_{42})$, $\bar{f}_{12} = -\frac{k_{42}(\sin\alpha_{142}+\sin\alpha_{143})}{l_{41}} + \frac{k_{42}\sin\alpha_{243}}{l_{42}}$, $\bar{f}_{21} = -\frac{k_{41}(\sin\alpha_{243}+\sin\alpha_{143})}{l_{43}} + \frac{k_{41}\sin\alpha_{142}}{l_{42}}$, $w_{11} = \frac{z_{42}^{\mathrm{T}}P_{z_{41}}(z_{12}+z_{13})}{l_{41}\sin\alpha_{142}}, w_{12} = \frac{z_{41}^{\mathrm{T}}P_{z_{42}}(z_{21}+z_{23})}{l_{42}\sin\alpha_{142}}, w_{21} = -\frac{z_{42}^{\mathrm{T}}P_{z_{43}}(z_{31}+z_{32})}{l_{43}\sin\alpha_{243}}, w_{22} = \frac{z_{43}^{\mathrm{T}}P_{z_{42}}(z_{21}+z_{23})}{l_{42}\sin\alpha_{243}} - \frac{z_{42}^{\mathrm{T}}P_{z_{43}}(z_{31}+z_{32})}{l_{43}\sin\alpha_{243}}$.

By considering a small neighborhood of the origin $\{e_1 = 0, e_2 = 0, e_{41} = 0, e_{42} = 0\}$, (66) can be linearized to

$$\dot{e}_4 = A_2 e_4 + B_2 e_s \quad (67)$$

where $A_2 = F_4(e_4)|_{e_4=0,e_s=0}$, and $B_2 = W(e_4)|_{e_4=0,e_s=0}$. Then, one has $\mathrm{tr}(A_2) = (-\bar{g}_1 - \bar{g}_2)|_{e_4=0,e_s=0} < 0$ and

$$\frac{\det(A_2)}{k_{41}k_{42}}|_{e_4=0,e_s=0} = \frac{\bar{g}_1\bar{g}_2 - \bar{f}_{12}\bar{f}_{21}}{k_{41}k_{42}}|_{e_4=0,e_s=0}$$
$$= \frac{l_{41}^*(\sin\alpha_{241}^*\sin\alpha_{342}^* + \sin^2\alpha_{342}^* + \sin\alpha_{342}^*\sin\alpha_{341}^*)}{l_{41}^*l_{42}^*l_{43}^*}$$
$$+ \frac{l_{43}^*(\sin\alpha_{241}^*\sin\alpha_{342}^* + \sin^2\alpha_{241}^* + \sin\alpha_{241}^*\sin\alpha_{341}^*)}{l_{42}^*l_{41}^*l_{43}^*}$$
$$- \frac{l_{42}^*(\sin\alpha_{241}^*\sin\alpha_{341}^* + \sin\alpha_{341}^*\sin\alpha_{342}^* + \sin^2\alpha_{341}^*)}{l_{41}^*l_{42}^*l_{43}^*}.$$

Then, if $\det(A_2) > 0$, one has that A_2 is Hurwitz. Similar to [20, Lemma 7], it can be observed that $\det(A_2) > 0$ if $l_{41}^* > l_{42}^*$ and $l_{43}^* > l_{42}^*$ hold. Based on the law of sines, the conditions $l_{41}^* > l_{42}^*$ and $l_{43}^* > l_{42}^*$ are equivalent to $\sin\alpha_{124}^* > \sin\alpha_{214}^*$ and $\sin\alpha_{423}^* > \sin\alpha_{234}^*$, respectively.

Combining (28) and (67), one has the linearized four-agent angle error dynamics

$$\dot{\bar{e}}_4 = \begin{bmatrix}\dot{e}_s\\ \dot{e}_4\end{bmatrix} = A_4\bar{e}_4 = \begin{bmatrix}A_1 & 0\\ B_2 & A_2\end{bmatrix}\begin{bmatrix}e_s\\ e_4\end{bmatrix}. \quad (68)$$

When A_1 and A_2 are Hurwitz, one has that A_4 is also Hurwitz. Then, for an arbitrary positive definite matrix $Q_3 \in \mathbb{R}^{4\times4}$, there always exists a positive definite matrix $P_3 \in \mathbb{R}^{4\times4}$ such that $-Q_3 = P_3A_4 + A_4^{\mathrm{T}}P_3$. Design the Lyapunov function candidate as

$$V_3 = \bar{e}_4^{\mathrm{T}}P_3\bar{e}_4$$

whose time derivative is

$$\dot{V}_3 = -\bar{e}_4^{\mathrm{T}}Q_3\bar{e}_4 \leq -\lambda_{\min}(Q_3)\|\bar{e}_4\|^2 \leq -\frac{\lambda_{\min}(Q_3)}{\lambda_{\max}(P_3)}V_3.$$

Then, one has

$$\|e_4\|^2 \leq \|\bar{e}_4\|^2 \leq \frac{V_3}{\lambda_{\min}(P_3)} \leq \frac{V_3(0)}{\lambda_{\min}(P_3)}e^{-\frac{\lambda_{\min}(Q_3)}{\lambda_{\max}(P_3)}t} \quad (69)$$

which implies that $\|e_4\|$ also exponentially converges to zero when the four agents' initial angle errors are in a small neighborhood of the origin $\{e_1 = 0, e_2 = 0, e_{41} = 0, e_{42} = 0\}$. To make the calculation of (65) valid and $W(e_4)$ well defined, one has to guarantee that $z_{41}(t) \neq \pm z_{42}(t), z_{42}(t) \neq \pm z_{43}(t)\,\forall t > 0$, which are equivalent to $\alpha_{142}(t) \neq 0, \pi$ and $\alpha_{243}(t) \neq 0, \pi\,\forall t > 0$, respectively. From (69), one has $|e_{41}(t)| \leq \sqrt{\frac{V_3(0)}{\lambda_{\min}(P_3)}}$, which implies

$$-\sqrt{\frac{V_3(0)}{\lambda_{\min}(P_3)}} + \alpha_{142}^* \leq \alpha_{142}(t) \leq \sqrt{\frac{V_3(0)}{\lambda_{\min}(P_3)}} + \alpha_{142}^*.$$

Therefore, if

$$\sqrt{V_3(0)} < \sqrt{\lambda_{\min}(P_3)} * \min\{\pi - \alpha_{142}^*, \alpha_{142}^*, \pi - \alpha_{243}^*, \alpha_{243}^*\}$$

one obtains $0 < \alpha_{142}(t) < \pi$ and $0 < \alpha_{243}(t) < \pi$, $\forall t > 0$, which guarantee the calculation of (65) valid since the first three agents are not collinear $\forall t > 0$. Then, according to (1) and (61), one has $\lim_{t\to\infty}\dot{p}_4(t) = \lim_{t\to\infty}u_{m4}(t) = \lim_{t\to\infty}[\mu_4(t)z_{41}(t) + (\mu_4(t) + \tilde{\mu}_4(t))z_{42}(t) + \tilde{\mu}_4(t)z_{43}(t)] = \lim_{t\to\infty}\dot{p}_4^*(t)$. By using (62)–(64), one has that the maneuvering defined in (13) is achieved. ■

To guarantee that $\|W(e_4)\|$ is bounded and control law (61) is well-defined, the collision between the agent 4 and agents 1 to 3 needs to be avoided. Similar to the three-agent formation case, we conduct the collision analysis by taking $l_{41}(t)$ as an example

$$l_{41}(t) = l_{41}(0) + \int_0^t z_{41}^{\mathrm{T}}(u_{f1} - u_{f4} + u_{m1} - u_{m4})\mathrm{d}\tau. \quad (70)$$

On the one hand, by using (32) and (69), one has

$$\int_0^t z_{41}^{\mathrm{T}}(u_{f1}-u_{f4})\mathrm{d}\tau \le \int_0^t 2(k_1|e_1|+k_{41}|e_{41}|+k_{42}|e_{42}|)d\tau$$
$$\le \int_0^t 2(k_1\sqrt{e_1^2+e_2^2}+\sqrt{2}\bar{k}_4\sqrt{e_{41}^2+e_{42}^2})d\tau$$
$$\le \frac{4k_1\lambda_{\max}(P_1)}{\lambda_{\min}(Q_1)}\sqrt{\frac{V_1(0)}{\lambda_{\min}(P_1)}}+\frac{4\bar{k}_4\lambda_{\max}(P_3)}{\lambda_{\min}(Q_3)}\sqrt{\frac{2\,V_3(0)}{\lambda_{\min}(P_3)}} \tag{71}$$

where $\bar{k}_4=\max\{k_{41},k_{42}\}$. On the other hand, by using (25) and (65), one has

$$\int_0^t z_{41}^{\mathrm{T}}(u_{m1}-u_{m4})\mathrm{d}\tau=\int_0^t s(\tau)l_{41}(\tau)\mathrm{d}\tau\ge 0 \tag{72}$$

when $s(t)>0$. For the case of $s(t)<0$, the conclusion can be similarly analyzed by following (48)–(49). Similarly, one has the following proposition.

Proposition 3: Consider a four-agent formation described by (1), with the control (12) for agents 1 to 3, the control (61) for the agent 4, and the mismatches $\mu_i(t),\tilde{\mu}_i(t),i=1,2,3$ as designed in (25), and $\mu_4(t),\tilde{\mu}_4(t)$ as designed in (65) and $s(t)>0$. If the initial angle errors $e_i(0),i=1,2,3$ and $e_{41}(0),e_{42}(0)$ are sufficiently small, $\alpha_i(0)\neq 0$, $\sin\alpha_{124}^*>\sin\alpha_{214}^*$, $\sin\alpha_{423}^*>\sin\alpha_{234}^*$, and $\alpha_{143}^*=\alpha_{142}^*+\alpha_{243}^*$. If $l_{41}(0)>\frac{4k_1\lambda_{\max}(P_1)}{\lambda_{\min}(Q_1)}\sqrt{\frac{V_1(0)}{\lambda_{\min}(P_1)}}+\frac{4\bar{k}_4\lambda_{\max}(P_3)}{\lambda_{\min}(Q_3)}\sqrt{\frac{2\,V_3(0)}{\lambda_{\min}(P_3)}}$, then no collision will happen between agents 4 and 1.

Now, we design a general formation maneuver control algorithm for arbitrary agent $i,4\le i\le N$

$$\begin{aligned}u_i=&-k_{i1}\left(\alpha_{j_1ij_2}-\alpha_{j_2ij_3}^*-\frac{\mu_i}{k_{i1}}\right)(z_{ij_1}+z_{ij_2})\\&-k_{i2}\left(\alpha_{j_2ij_3}-\alpha_{j_2ij_3}^*-\frac{\tilde{\mu}_i}{k_{i2}}\right)(z_{ij_2}+z_{ij_3})\\=&-k_{i1}(\alpha_{j_1ij_2}-\alpha_{j_1ij_2}^*)(z_{ij_1}+z_{ij_2})-k_{i2}(\alpha_{j_2ij_3}-\alpha_{j_2ij_3}^*)\\&\times(z_{ij_2}+z_{ij_3})+\mu_i z_{ij_1}+(\mu_i+\tilde{\mu}_i)z_{ij_2}+\tilde{\mu}_i z_{ij_3}\\=&\,u_{fi}+u_{mi}\end{aligned} \tag{73}$$

where $\mu_i(t),\tilde{\mu}_i(t)$ can be similarly designed according to (62)–(65), and $j_1,j_2,j_3<i$. Under the fact that the four-agent formation achieves the desired shape exponentially, we suppose for a $4<k<N$, the k-agent formation converges to the desired shape exponentially. We need to prove that for the $(k+1)$-agent formation, the angle errors $e_{(k+1)1}=\alpha_{j_1(k+1)j_2}-\alpha_{j_1(k+1)j_2}^*$ and $e_{(k+1)2}=\alpha_{j_2(k+1)j_3}-\alpha_{j_2(k+1)j_3}^*$ converges to zero exponentially. Similar to the proof from (60) to (69), one has that the angle errors $e_{(k+1)1}$ and $e_{(k+1)2}$ exponentially converge to zero. Therefore, the control algorithm (73) can locally stabilize agent $k+1$, i.e., the $(k+1)$-agent formation converges to the desired shape exponentially. So, by using induction, the N-agent formation converges to the desired formation shape exponentially. Similarly, the formation maneuvering is achieved since $\lim_{t\to\infty}\dot{p}_i(t)=\lim_{t\to\infty}u_{mi}(t)=\lim_{t\to\infty}\dot{p}_i^*(t)$.

B. Measurement-Independent Mismatches

Similar to the design procedure (62)–(65), we use the measurement-independent mismatches to realize the desired maneuvering under the measurements of $z_{4i},i=1,2,3$. The information of the desired formation shape p^{b*} described in $\sum_{b(0)}$ is required to be known in the mismatch design stage.

By applying translation, rotation, and scaling, simultaneously, one has

$$\mu_4 z_{41}^{b*}+(\mu_4+\tilde{\mu}_4)z_{42}^{b*}+\tilde{\mu}_4 z_{43}^{b*}=v_c^{b*}+\omega^* E p_{c4}^{b*}+s(t)p_{c4}^{b*} \tag{74}$$

where $z_{4j}^{b*}=\frac{p_j^{b*}-p_4^{b*}}{\|p_j^{b*}-p_4^{b*}\|}$. Then, mismatches μ_4 and $\tilde{\mu}_4$ can be calculated by

$$\begin{bmatrix}\mu_4\\ \tilde{\mu}_4\end{bmatrix}=[z_{41}^{b*}+z_{42}^{b*}\,z_{42}^{b*}+z_{43}^{b*}]^{-1}(v_c^{b*}+\omega^* E p_{c4}^{b*}+s(t)p_{c4}^{b*}) \tag{75}$$

which is well defined when $[z_{41}^{b*}+z_{42}^{b*}\,z_{42}^{b*}+z_{43}^{b*}]^{-1}$ is invertible. Since no three points are collinear in the desired generically angle rigid formation [20, Definition 4], the matrix $[z_{41}^{b*}+z_{42}^{b*}\,z_{42}^{b*}+z_{43}^{b*}]$ is invertible. Now, we present the main result.

Theorem 4: Consider a four-agent formation described by (1), with the control (12) for agents 1 to 3, the control (61) for the agent 4, and the mismatches $\mu_i,\tilde{\mu}_i,i=1,2,3$ as designed in (38), and μ_4 and $\tilde{\mu}_4$ as designed in (75). If the initial angle error $e_i(0),i=1,\ldots,3,e_{41}(0),e_{42}(0)$ and the designed-mismatches are sufficiently small, $\alpha_i(0)\neq 0$ and $\|p_i(0)-p_j(0)\|,i\neq j$ are sufficiently away from zero and $\sin\alpha_{124}^*>\sin\alpha_{214}^*,\sin\alpha_{423}^*>\sin\alpha_{234}^*$, and $\alpha_{143}^*=\alpha_{142}^*+\alpha_{243}^*$, then the four-agent formation converges exponentially to its desired shape and maneuvers with the prescribed translation (35), rotation (5), and scaling (6) simultaneously.

Proof: Using similar steps as Appendix B, one has agent 4's angle error dynamics under the control (61) and (75)

$$\begin{aligned}\dot{e}_4=&F_4(e_4)e_4+W(e_4)e_s+H_4(e_4)U_4\\=&\begin{bmatrix}-\bar{g}_1 & \bar{f}_{12}\\ \bar{f}_{21} & -\bar{g}_2\end{bmatrix}\begin{bmatrix}\alpha_{142}-\alpha_{142}^*\\ \alpha_{243}-\alpha_{243}^*\end{bmatrix}+\begin{bmatrix}w_{11} & w_{12}\\ w_{21} & w_{22}\end{bmatrix}\begin{bmatrix}e_1\\ e_2\end{bmatrix}\\&+\begin{bmatrix}h_{11} & h_{12} & h_{13} & h_{14} & h_{15} & h_{16} & h_{17} & h_{18}\\ h_{21} & h_{22} & h_{23} & h_{24} & h_{25} & h_{26} & h_{27} & h_{28}\end{bmatrix}U_4\end{aligned} \tag{76}$$

where e_4, $F_4(e_4)$, and $W(e_4)$ have the same definitions as (66), $U_4=[\mu_1,\mu_2,\mu_3,\mu_4,\tilde{\mu}_1,\tilde{\mu}_2,\tilde{\mu}_3,\tilde{\mu}_4]^{\mathrm{T}}$, and $h_{11}=-z_{42}^{\mathrm{T}}\frac{P_{z_{41}}}{l_{41}\sin\alpha_{142}}z_{12}$, $h_{12}=-z_{41}^{\mathrm{T}}\frac{P_{z_{42}}}{l_{42}\sin\alpha_{142}}z_{23}$, $h_{13}=0$, $h_{14}=z_{42}^{\mathrm{T}}\frac{P_{z_{41}}}{l_{41}\sin\alpha_{142}}z_{42}+z_{41}^{\mathrm{T}}\frac{P_{z_{42}}}{l_{42}\sin\alpha_{142}}z_{41}$, $h_{15}=-z_{42}^{\mathrm{T}}\frac{P_{z_{41}}}{l_{41}\sin\alpha_{142}}z_{13}$, $h_{16}=-z_{41}^{\mathrm{T}}\frac{P_{z_{42}}}{l_{42}\sin\alpha_{142}}z_{21}$, $h_{17}=0$, $h_{18}=z_{42}^{\mathrm{T}}\frac{P_{z_{41}}}{l_{41}\sin\alpha_{142}}(z_{42}+z_{43})+z_{41}^{\mathrm{T}}\frac{P_{z_{42}}}{l_{42}\sin\alpha_{142}}z_{43}$, $h_{21}=0$, $h_{22}=-z_{43}^{\mathrm{T}}\frac{P_{z_{42}}}{l_{42}\sin\alpha_{243}}z_{23}$, $h_{23}=-z_{42}^{\mathrm{T}}\frac{P_{z_{43}}}{l_{43}\sin\alpha_{243}}z_{31}$, $h_{24}=z_{42}^{\mathrm{T}}\frac{P_{z_{43}}}{l_{43}\sin\alpha_{243}}(z_{41}+z_{42})+z_{43}^{\mathrm{T}}\frac{P_{z_{42}}}{l_{42}\sin\alpha_{243}}z_{41}$, $h_{25}=0$, $h_{26}=-z_{43}^{\mathrm{T}}\frac{P_{z_{42}}}{l_{42}\sin\alpha_{243}}z_{21}$, $h_{27}=-z_{42}^{\mathrm{T}}\frac{P_{z_{43}}}{l_{43}\sin\alpha_{243}}z_{32}$, and $h_{28}=z_{42}^{\mathrm{T}}\frac{P_{z_{43}}}{l_{43}\sin\alpha_{243}}z_{42}+z_{43}^{\mathrm{T}}\frac{P_{z_{42}}}{l_{42}\sin\alpha_{243}}z_{43}$.

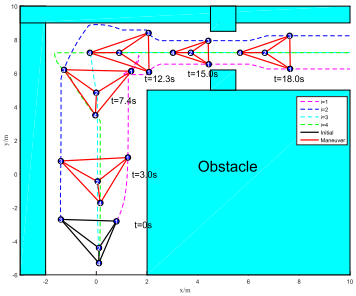

Fig. 5. Formation maneuvering trajectories under measurement-dependent mismatches.

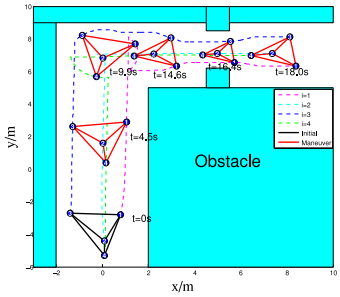

Fig. 7. Formation maneuvering trajectories under measurement-independent mismatches.

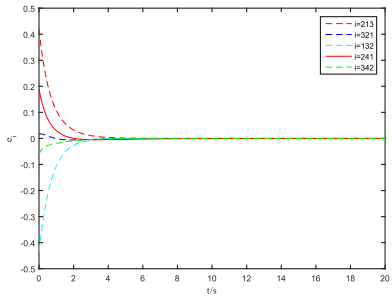

Fig. 6. Evolution of angle errors under measurement-dependent mismatches.

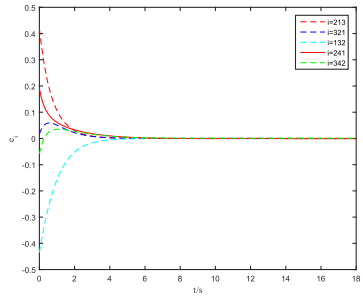

Fig. 8. Evolution of angle errors under measurement-independent mismatches.

Note that $\|e_s\|$ and $\|U_4\|$ are sufficiently small. Therefore, the angle error dynamics (76) are locally stable when $F_4(e_4)|_{e_4=0}$ is Hurwitz. To obtain the local stability of (76), by using the similar analysis steps from (67) to (72), one has the local stability of angle error dynamics (76). Also, when the initial angle errors are sufficiently small and the initial distances are sufficiently away from zero, no collision will happen. Similarly, it can be proved that the prescribed formation maneuvering in terms of translation, rotation, and scaling can be achieved. For agents $4 < i \leq N$, the formation maneuver algorithm (73) with measurement-independent mismatches can be similarly designed according to (65). ■

Remark 5: Note that since $p_i^b - p_j^b = p_i - p_c - (p_j - p_c) = p_i - p_j$, the maneuvering reference point p_c can be set as other well-selected point of interest, which is not necessary the centroid of the formation.

V. Simulation Examples

In this section, to verify the effectiveness of the proposed formation maneuver control algorithms, we present numerical simulation examples by conducting four-agent obstacle avoidance task. The desired angles describing the formation shape are set as $\alpha_1^* = \pi/4$, $\alpha_2^* = \pi/2$, $\alpha_3^* = \pi/4$, $\alpha_{142}^* = \arctan 0.5$, and $\alpha_{243}^* = \arctan 0.5$. The initial states of all agents are $p_1(0) = [0.8; -3.2]$, $p_2(0) = [0.1; -4.4]$, $p_3(0) = [-1.4; -3.3]$, and $p_4(0) = [0.1; -5.3]$. A reference formation configuration in $\sum_g$ is $p_1^* = [0.9619; 4.6234]$, $p_2^* = [-0.1706; 3.1289]$, $p_3^* = [-1.6666; 4.2629]$, and $p_4^* = [0.0134; 1.8154]$, which satisfies all the desired angle constraints. All the control gains are set as $k_i = 1, i = 1, 2, 3$, $k_{41} = k_{42} = 1$. For the case of measurement-dependent mismatches, the maneuvering command velocity is $v_c^* = [0; 1.2], t \in [0, 9]$; $v_c^* = [1; 0], t \in [11, 20]$; $\omega^* = -\frac{\pi}{8}, t \in [7, 11]$; $s(t) = -0.8e^{-0.4(t-12)}, t \in [12, 13]$; and $s(t) = 0.8e^{-0.4(t-16)}, t \in [16.5, 17]$. The simulation results are given in Figs. 5 and 6.

For the case of measurement-independent mismatches, the maneuvering command velocity is $v_c^{b*} = [-0.5795; -0.9933], t \in [0, 9]$; $v_c^{b*} = [-1.2957; 0.7558]$, $t \in [13, 20]$; $\omega^* = -\pi/8, t \in [9, 13]$; $s(t) = -0.4e^{-0.4(t-12)}, t \in [14, 15]$; and $s(t) = 0.4e^{-0.4(t-12)}, t \in [16.5, 17]$. The corresponding simulation results are given in Figs. 7 and 8.

According to the aforementioned simulation results, one obtains that in both of the measurement-dependent and measurement-independent mismatch cases, the translation, rotation, and scaling maneuvering can be conducted simultaneously. The angle errors converge to zero in both cases. Note that in the measurement-independent mismatch case, only bearing measurements are needed. As corresponds to Remark 3, the translational maneuvering command velocities are different in these two cases, but the rotational and scaling maneuvering are not influenced.

VI. Conclusion and Future Works

This article has realized the formation maneuver control by using a designed-mismatch angle approach. The formation is described by angles and constructed from a triangular shape and grown with two angle constraints for each newly added agent. Two types of designed mismatches have been investigated: measurement-dependent case and measurement-independent case. For both cases, the formation maneuver control algorithms have been proposed to realize the desired

maneuvering. To analyze the stability of the angle errors, the angle error dynamics have been derived by using the dot product of two bearings. Future work will focus on formation maneuver control of multiagent systems with double-integrator dynamics.

APPENDIX A

For Section III-B, we use the dot product of two bearings to obtain the angle error dynamics. In the following, we consider the maneuvering of translation, rotation, and scaling simultaneously. Take agent 1 as an example

$$\frac{\mathrm{d}(\cos\alpha_1)}{\mathrm{d}t} = -\sin(\alpha_1)\dot{\alpha}_1 = \frac{\mathrm{d}(z_{12}^{\mathrm{T}} z_{13})}{\mathrm{d}t} = (\dot{z}_{12})^{\mathrm{T}} z_{13} + (z_{12})^{\mathrm{T}} \dot{z}_{13}. \tag{77}$$

Considering that for $x \in \mathbb{R}^2, x \neq 0$, $\frac{\mathrm{d}}{\mathrm{d}t}(\frac{x}{\|x\|}) = \frac{I_2 - \frac{x}{\|x\|}\frac{x^{\mathrm{T}}}{\|x\|}}{\|x\|}\dot{x}$ and denoting $P_{x/\|x\|} = I_2 - \frac{x}{\|x\|}\frac{x^{\mathrm{T}}}{\|x\|}$, one has $\dot{z}_{12} = \frac{P_{z_{12}}}{l_{12}}(\dot{p}_2 - \dot{p}_1)$. By using (12), one has

$$\begin{aligned}\dot{z}_{12} &= \frac{P_{z_{12}}}{l_{12}}(u_2 - u_1) \\ &= \frac{P_{z_{12}}}{l_{12}}[-k_2(\alpha_2 - \alpha_2^*)(z_{23} + z_{21}) + \mu_2(t) z_{23} + \tilde{\mu}_2(t) z_{21} \\ &\quad + k_1(\alpha_1 - \alpha_1^*)(z_{13} + z_{12}) - \mu_1(t) z_{12} - \tilde{\mu}_1(t) z_{13}].\end{aligned} \tag{78}$$

From (25), one has

$$\begin{aligned}&\mu_2(t) z_{23} + \tilde{\mu}_2(t) z_{21} - \mu_1(t) z_{12} - \tilde{\mu}_1(t) z_{13} \\ &= v_c^* + (\omega^* E + s(t) I_2) p_{c2} - v_c^* - (\omega^* E + s(t) I_2) p_{c1} \\ &= (\omega^* E + s(t) I_2)\,(p_{c2} - p_{c1}).\end{aligned} \tag{79}$$

Substituting (79) into (78) yields

$$\begin{aligned}&(\dot{z}_{12})^{\mathrm{T}} z_{13} \\ &= [k_1(\alpha_1 - \alpha_1^*)(z_{13} + z_{12}) - k_2(\alpha_2 - \alpha_2^*)(z_{23} + z_{21}) \\ &\quad + (\omega^* E + s(t) I_2)(p_{c2} - p_{c1})]^{\mathrm{T}} \frac{P_{z_{12}}}{l_{12}} z_{13} \\ &= \frac{1}{l_{12}}[k_1(\sin^2\alpha_1)(\alpha_1 - \alpha_1^*) - k_2(\sin\alpha_1 \sin\alpha_2)(\alpha_2 - \alpha_2^*)] \\ &\quad - \omega^* z_{12}^{\mathrm{T}} E P_{z_{21}} z_{13}\end{aligned} \tag{80}$$

where we have used the fact that $P_x x = 0$ for all $x \in \mathbb{R}^2$ and $s(t) l_{12} z_{12}^{\mathrm{T}} P_{z_{21}} z_{13} = 0$. Since $x^{\mathrm{T}} E x = 0$ for all $x \in \mathbb{R}^2$, one has $-\omega^* z_{12}^{\mathrm{T}} E P_{z_{21}} z_{13} = -\omega^* z_{12}^{\mathrm{T}} E z_{13}$. Similarly, one can get

$$\begin{aligned}(z_{12})^{\mathrm{T}} \dot{z}_{13} = \omega^* z_{12}^{\mathrm{T}} E z_{13} + \frac{1}{l_{13}}[k_1(\sin^2\alpha_1)(\alpha_1 - \alpha_1^*) \\ - k_3(\cos\alpha_2 + \cos\alpha_1 \cos\alpha_3)(\alpha_3 - \alpha_3^*)].\end{aligned} \tag{81}$$

Substituting (80) and (81) into (77), one has the angle error dynamics of the agent 1

$$\begin{aligned}\dot{\alpha}_1 = &-(\sin\alpha_1)\left(\frac{k_1}{l_{12}} + \frac{k_1}{l_{13}}\right)(\alpha_1 - \alpha_1^*) + k_2 \frac{\sin\alpha_2}{l_{12}}(\alpha_2 - \alpha_2^*) \\ &+ k_3 \frac{\sin\alpha_3}{l_{13}}(\alpha_3 - \alpha_3^*).\end{aligned} \tag{82}$$

By using the same analysis steps, one has

$$\begin{aligned}\dot{\alpha}_2 = &-(\sin\alpha_2)\left(\frac{k_2}{l_{21}} + \frac{k_2}{l_{23}}\right)(\alpha_2 - \alpha_2^*) + k_1 \frac{\sin\alpha_1}{l_{21}}(\alpha_1 - \alpha_1^*) \\ &+ k_3 \frac{\sin\alpha_3}{l_{23}}(\alpha_3 - \alpha_3^*)\end{aligned} \tag{83}$$

$$\begin{aligned}\dot{\alpha}_3 = &-(\sin\alpha_3)\left(\frac{k_3}{l_{31}} + \frac{k_3}{l_{32}}\right)(\alpha_3 - \alpha_3^*) \\ &+ k_1 \frac{\sin\alpha_1}{l_{31}}(\alpha_1 - \alpha_1^*) + k_2 \frac{\sin\alpha_2}{l_{32}}(\alpha_2 - \alpha_2^*).\end{aligned} \tag{84}$$

Writing (82)–(84) into a compact form, one has the overall angle error dynamics (26), which are independent of the mismatches $\mu_i(t)$ and $\tilde{\mu}_i(t)$.

APPENDIX B

For Section IV-A, we use a similar approach to obtain the angle error dynamics of e_{41} and e_{42} for the agent 4 under the control algorithm (61). In the following, we consider the maneuvering of translation, rotation, and scaling simultaneously.

By using (12) and (61), one has

$$\dot{z}_{41} = \frac{P_{z_{41}}}{l_{41}}(\dot{p}_1 - \dot{p}_4) = \frac{P_{z_{41}}}{l_{41}}(u_{f1} - u_{f4} + u_{m1} - u_{m4}).$$

By substituting the definitions of u_{fi} and u_{mi}, one has

$$\begin{aligned}&z_{42}^T \frac{P_{z_{41}}}{l_{41}}(u_{f1} - u_{f4}) \\ &= \frac{-z_{42}^{\mathrm{T}} P_{z_{41}}(z_{12} + z_{13}) e_1 + k_{41}(\alpha_{142} - \alpha_{142}^*)\sin^2\alpha_{142}}{l_{41}} \\ &\quad + \frac{k_{42}(\alpha_{243} - \alpha_{243}^*)(\sin\alpha_{142})(\sin\alpha_{142} + \sin\alpha_{143})}{l_{41}}.\end{aligned} \tag{85}$$

On the other hand, one has

$$\begin{aligned}z_{42}^T \frac{P_{z_{41}}}{l_{41}}(u_{m1} - u_{m4}) &= \frac{z_{42}^T P_{z_{41}}(\omega^* E + s(t) I_2)(p_1 - p_4)}{l_{41}} \\ &= \omega^* z_{42}^{\mathrm{T}} E z_{41}\end{aligned} \tag{86}$$

where we have used the fact that $P_{z_{41}} z_{41} = 0$ and $z_{41}^T E z_{41} = 0$. Similarly, one also has

$$\begin{aligned}z_{41}^{\mathrm{T}} \dot{z}_{42} &= z_{41}^{\mathrm{T}} \frac{P_{z_{42}}}{l_{42}}(u_{f2} - u_{f4} + u_{m2} - u_{m4}) \\ &= \frac{-z_{41}^{\mathrm{T}} P_{z_{42}}(z_{21} + z_{23}) e_2 + k_{41}(\alpha_{142} - \alpha_{142}^*)\sin^2\alpha_{142}}{l_{42}} \\ &\quad + \frac{k_{42}(\alpha_{243} - \alpha_{243}^*)(-\sin\alpha_{142}\sin\alpha_{243})}{l_{42}} \\ &\quad + \omega^* z_{41}^{\mathrm{T}} E z_{42}.\end{aligned} \tag{87}$$

By substituting (85)–(87) into $\dot{\alpha}_{142} = -(z_{42}^{\top}\dot{z}_{41} + z_{41}^{\top}\dot{z}_{42})/\sin\alpha_{142}$, one has the dynamics of α_{142} as

$$\begin{aligned}\dot{\alpha}_{142} = &-(\sin\alpha_{142})\left(\frac{k_{41}}{l_{41}} + \frac{k_{41}}{l_{42}}\right)(\alpha_{142} - \alpha_{142}^*) \\ &- \frac{k_{42}(\alpha_{243} - \alpha_{243}^*)(\sin\alpha_{142} + \sin\alpha_{143})}{l_{41}}\end{aligned}$$

$$+\frac{k_{42}(\alpha_{243}-\alpha^*_{243})\sin\alpha_{243}}{l_{42}}+\frac{z_{41}^{\mathrm{T}}P_{z_{42}}(z_{21}+z_{23})e_2}{l_{42}\sin\alpha_{142}}$$
$$+\frac{z_{42}^{\mathrm{T}}P_{z_{41}}(z_{12}+z_{13})e_1}{l_{41}\sin\alpha_{142}}. \tag{88}$$

By using the same analysis approach, one has the angle error dynamics of α_{243} as

$$\dot{\alpha}_{243}=-(\sin\alpha_{243})\left(\frac{k_{42}}{l_{43}}+\frac{k_{42}}{l_{42}}\right)(\alpha_{243}-\alpha^*_{243})-\frac{u_{f2}^{\mathrm{T}}P_{z_{42}}z_{43}}{l_{42}\sin\alpha_{243}}$$
$$-\frac{k_{41}(\alpha_{142}-\alpha^*_{142})(\sin\alpha_{243}+\sin\alpha_{143})}{l_{43}}$$
$$+\frac{k_{41}(\alpha_{142}-\alpha^*_{142})\sin\alpha_{142}}{l_{42}}-\frac{u_{f3}^{\mathrm{T}}P_{z_{43}}z_{42}}{l_{43}\sin\alpha_{243}}. \tag{89}$$

By combining (88) and (89), one has the angle error dynamics given in (66), which are independent of the designed mismatches $\mu_i(t), \tilde{\mu}_i, i=1,\ldots,4$.

REFERENCES

[1] B. D. Anderson, B. Fidan, C. Yu, and D. Walle, "UAV formation control: Theory and application," in *Proc. Recent Adv. Learn. Control*, 2008, pp. 15–33.

[2] H. Bai and J. T. Wen, "Cooperative load transport: A formation-control perspective," *IEEE Trans. Robot.*, vol. 26, no. 4, pp. 742–750, Aug. 2010.

[3] G.-P. Liu and S. Zhang, "A survey on formation control of small satellites," *Proc. IEEE*, vol. 106, no. 3, pp. 440–457, Mar. 2018.

[4] K.-K. Oh, M.-C. Park, and H.-S. Ahn, "A survey of multi-agent formation control," *Automatica*, vol. 53, pp. 424–440, 2015.

[5] Z. Lin, B. Francis, and M. Maggiore, "Necessary and sufficient graphical conditions for formation control of unicycles," *IEEE Trans. Autom. Control*, vol. 50, no. 1, pp. 121–127, Jan. 2005.

[6] M. Cao, C. Yu, and B. D. Anderson, "Formation control using range-only measurements," *Automatica*, vol. 47, no. 4, pp. 776–781, 2011.

[7] S. Zhao and D. Zelazo, "Bearing rigidity and almost global bearing-only formation stabilization," *IEEE Trans. Autom. Control*, vol. 61, no. 5, pp. 1255–1268, May 2016.

[8] S. Zhao and D. Zelazo, "Translational and scaling formation maneuver control via a bearing-based approach," *IEEE Control Netw. Syst.*, vol. 4, no. 3, pp. 429–438, Sep. 2017.

[9] W. Ren, "Multi-vehicle consensus with a time-varying reference state," *Syst. Control Lett.*, vol. 56, no. 7-8, pp. 474–483, 2007.

[10] H. G. de Marina, B. Jayawardhana, and M. Cao, "Distributed rotational and translational maneuvering of rigid formations and their applications," *IEEE Trans. Robot.*, vol. 32, no. 3, pp. 684–697, Jun. 2016.

[11] Z. Sun, S. Mou, B. D. Anderson, and A. S. Morse, "Rigid motions of 3-D undirected formations with mismatch between desired distances," *IEEE Trans. Autom. Control*, vol. 62, no. 8, pp. 4151–4158, 2017.

[12] S. Zhao, "Affine formation maneuver control of multiagent systems," *IEEE Trans. Autom. Control*, vol. 63, no. 12, pp. 4140–4155, Dec. 2018.

[13] T. Han, Z. Lin, R. Zheng, and M. Fu, "A barycentric coordinate-based approach to formation control under directed and switching sensing graphs," *IEEE Trans. Cybern.*, vol. 48, no. 4, pp. 1202–1215, Apr. 2018.

[14] Z. Lin, W. Ding, G. Yan, C. Yu, and A. Giua, "Leader-follower formation via complex Laplacian," *Automatica*, vol. 49, no. 6, pp. 1900–1906, 2013.

[15] Z. Han, L. Wang, Z. Lin, and R. Zheng, "Formation control with size scaling via a complex Laplacian-based approach," *IEEE Trans. Cybern.*, vol. 46, no. 10, pp. 2348–2359, Oct. 2016.

[16] X. Li and L. Xie, "Dynamic formation control over directed networks using graphical Laplacian approach," *IEEE Trans. Autom. Control*, vol. 63, no. 11, pp. 3761–3774, Nov. 2018.

[17] S. Coogan and M. Arcak, "Scaling the size of a formation using relative position feedback," *Automatica*, vol. 48, no. 10, pp. 2677–2685, 2012.

[18] S. Zhao and D. Zelazo, "Bearing rigidity theory and its applications for control and estimation of network systems: Life beyond distance rigidity," *IEEE Control Syst. Mag.*, vol. 39, no. 2, pp. 66–83, Apr. 2019.

[19] M. H. Trinh, S. Zhao, Z. Sun, D. Zelazo, B. D. Anderson, and H.-S. Ahn, "Bearing-based formation control of a group of agents with leader-first follower structure," *IEEE Trans. Autom. Control*, vol. 64, no. 2, pp. 598–613, Feb. 2019.

[20] L. Chen, M. Cao, and C. Li, "Angle rigidity and its usage to stabilize multi-agent formations in 2D," *IEEE Trans. Autom. Control*, to be published, doi: 10.1109/TAC.2020.3025539.

[21] M. Basiri, A. N. Bishop, and P. Jensfelt, "Distributed control of triangular formations with angle-only constraints," *Syst. Control Lett.*, vol. 59, no. 2, pp. 147–154, 2010.

[22] H. Goldstein, *Classical Mechanics*. Reading, MA, USA: Addison-Wesley, 1980.

[23] L. Chen, M. Cao, H. G. De Marina, Y. Guo, and Y. Kapitanyuk, "Triangular formation maneuver using designed mismatched angles," in *Proc. Eur. Control Conf.*, 2019, pp. 1544–1549.

[24] H. K. Khalil, *Nonlinear Systems*, 3rd ed. Upper Saddle River, NJ, USA: Prentice-Hall, 2002.

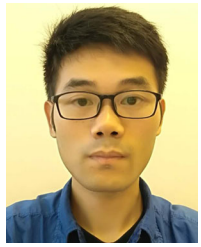

Liangming Chen (Graduate Student Member, IEEE) received the B. E. degree in automation from Southwest Jiaotong University, Chengdu, China, in 2015. He is currently working toward the joint Ph.D. degree with the Harbin Institute of Technology, Harbin, China and the University of Groningen, Groningen, The Netherlands.

His current research interests include rigidity theory, formation control, and multiagent systems.

Hector Garcia de Marina (Member, IEEE) received the M.Sc. degree in electronics engineering from the Complutense University of Madrid, Madrid, Spain, in 2008, the M.Sc. degree in control engineering from the University of Alcala, Alcala de Henares, Spain, in 2011, and the Ph.D. degree in systems and control from the University of Groningen, Groningen, The Netherlands, in 2016.

He was a Postdoctoral with the École Nationale de l'Aviation Civile, Toulouse, France, from 2016 to 2018. From 2018 to 2020, he was an Assistant Professor with the Unmanned Aerial Systems Center, University of Southern Denmark, Odense, Denmark. Since 2020, he has been a Research Fellow with the Complutense University of Madrid. His research interests include the guidance navigation and control for autonomous robots, and multiagent systems.

Ming Cao (Senior Member, IEEE) received the bachelor's and master's degrees in electrical engineering from Tsinghua University, Beijing, China, in 1999 and 2002, respectively, and the Ph.D. degree in electrical engineering from Yale University, New Haven, CT, USA, in 2007.

He is currently a Professor of systems and control with the Engineering and Technology Institute, University of Groningen, Groningen, Netherlands, where he started as an Assistant Professor in 2008. From 2007 to 2008, he was a Postdoctoral Research Associate with the Department of Mechanical and Aerospace Engineering, Princeton University, Princeton, NJ, USA. He worked as a Research Intern with the Mathematical Sciences Department, IBM T. J. Watson Research Center, Ossining, NY, USA, in 2006. His main research interests include autonomous agents and multiagent systems, decision-making dynamics, and complex networks.

Dr. Cao was the recipient of the 2017 and inaugural recipient of the Manfred Thoma Medal from the International Federation of Automatic Control and the 2016 European Control Award sponsored by the European Control Association. He is a Senior Editor for the *Systems and Control Letters*, an Associate Editor for the IEEE TRANSACTIONS ON AUTOMATIC CONTROL, IEEE TRANSACTIONS ON CIRCUITS AND SYSTEMS, and *IEEE Circuits and Systems Magazine*.